Phil. Trans. R. Soc. Lond. B **304**, 255–272 (1984) [255]

Printed in Great Britain

MAPPING OF CYTOCHROME OXIDASE PATCHES AND OCULAR DOMINANCE COLUMNS IN HUMAN VISUAL CORTEX

BY J. C. HORTON[1]† AND E. TESSA HEDLEY-WHYTE[2]

[1]*Department of Neurobiology, Harvard Medical School, 25 Shattuck Street, Boston, Massachusetts, 02115, U.S.A. and* [2]*C. S. Kubik Laboratory of Neuropathology, Massachusetts General Hospital and Department of Pathology, Harvard Medical School, Boston, Massachusetts, 02115, U.S.A.*

(*Communicated by T. N. Wiesel, For.Mem.R.S. – Received 28 February* 1983)

[Plates 1–14]

CONTENTS

PAGE

1. INTRODUCTION 256

2. MATERIALS AND METHODS 257

3. RESULTS 258
   (*a*) Cytochrome oxidase staining in normal human striate cortex 258
   (*b*) Effect of eye removal on cytochrome oxidase staining in human lateral geniculate nucleus 259
   (*c*) Effect of eye removal upon cytochrome oxidase staining in human striate cortex 260
      (i) Appearance of ocular dominance columns in layer IV 261
      (ii) Effect of eye removal on the cytochrome oxidase patches 262
      (iii) Secondary transneuronal anterograde degeneration in the cortex 262
      (iv) Pattern formed by ocular dominance columns in human striate cortex 264
   (*d*) Normal development of the patches in striate cortex 266

4. DISCUSSION 267
   (*a*) Comparison between macaque and human striate cortex 267
   (*b*) Significance for neuropathology 269
   (*c*) Development of patches in human striate cortex 270

5. REFERENCES 271

The cytochrome oxidase stain was applied to autopsy specimens of human brain. In primary visual cortex patches of darker enzyme staining were present in layers II, III, IVb, V, and VI. The patches were oval, about 400 by 250 μm, with a density of one patch per 0.6–0.8 mm² of cortex. They were organized into rows spaced about

† To whom all correspondence should be sent.

The Royal Society is collaborating with JSTOR to digitize, preserve, and extend access to *Philosophical Transactions of the Royal Society of London. Series B, Biological Sciences.* www.jstor.org

1 mm apart, intersecting the 17–18 border at right angles. The patches also stained preferentially for AChE activity.

The lateral geniculate body was examined in two patients who died many years after losing one eye as adults. In atrophied laminae cytochrome oxidase activity was severely reduced.

In the visual cortex from three cases after monocular enucleation, regular alternating light and dark columns of cytochrome oxidase activity were visible in layer IVc, presumably corresponding to ocular dominance columns. In two cases their pattern was reconstructed over 200–400 mm^2 of striate cortex. The columns appeared as roughly parallel slabs about 1 mm wide, oriented perpendicular to the 17–18 border as in the macaque. In the upper layers light and dark rows of patches were present, which fit in register with the light and dark ocular dominance columns below. In layer IV the ocular dominance columns were also visible in Nissl stained sections as a consequence of secondary anterograde transneuronal degeneration. Darker Nissl stained columns matched lighter cytochrome oxidase stained columns corresponding to the missing eye. Quantitative measurements demonstrated a 10% loss of mean cell area and 35% increase in cell density in ocular dominance columns belonging to the missing eye, which accounts for their darker appearance in the Nissl stain.

Patches were not present in a foetus at six months gestation. However, they were clearly formed in a six month old baby, although they appeared smaller and more closely spaced than in the adult.

These results show that patches are present in man, in addition to other primates, although they appear proportionately larger. Ocular dominance columns are also present, in common with certain species of primates like the macaque, baboon and galago. Cytochrome oxidase histochemistry promises to be a useful technique for mapping anatomical features of the human brain *post mortem*.

1. Introduction

In the macaque monkey afferents from left and right eye laminae of the lateral geniculate nucleus segregate in layer IVc of striate cortex to form ocular dominance columns. These columns have been demonstrated by Fink–Heimer staining after placing lesions in single geniculate laminae, [^{3}H]proline transneuronal radioautography, and [^{14}C]-2-deoxyglucose mapping of monocularly stimulated monkeys (Hubel & Wiesel 1972; Wiesel *et al.* 1974; Kennedy *et al.* 1976). None of these methods can be applied in man. However, the ocular dominance columns in macaque striate cortex can also be shown using the Liesegang stain, a reduced silver technique derived from Cajal (LeVay *et al.* 1975). It reveals a regular pattern of thin pale bands in layer IV that straddle the borders of the ocular dominance columns. Recently Hitchcock & Hickey (1980) have discovered a pattern of regular bands in *post mortem* specimens of normal human striate cortex using the Glees silver stain. The bands appear similar to the Liesegang pattern in the macaque, but more widely spaced. This finding implies that ocular dominance columns may be present in the human brain.

Wong-Riley (1978, 1979, 1980) has introduced the use of cytochrome oxidase histochemistry for mapping metabolic activity in the mammalian nervous system. In striate cortex from normal monkeys the cytochrome oxidase stain shows a regular, patchy distribution of enzyme activity, most prominent in layers II and III (Horton & Hubel 1980*a*, 1980*b*, 1981; Humphrey & Hendrickson 1980; Hendrickson *et al.* 1981). These patches also stain preferentially for glutamic acid decarboxylase (Hendrickson *et al.* 1981), acetylcholinesterase (AChE), lactate dehydrogenase, succinate dehydrogenase (Horton 1984), and myelin (Horton 1983; Tootell *et al.*

1983). Furthermore, each patch in layers II and III receives a direct projection from the lateral geniculate nucleus (Horton 1984; Fitzpatrick *et al.* 1983) and is organized into a system of rows, each lying in register with an ocular dominance column in layer IVc. The latter point was demonstrated by removing one eye in a macaque monkey, waiting 10 d, and then staining striate cortex for cytochrome oxidase (Horton & Hubel 1981; Horton 1984). In layer IVc loss of cytochrome oxidase staining occurred in ocular dominance columns corresponding to the missing eye, causing a pattern of alternating light and dark columns to appear. In the upper layers, more lightly staining rows of patches lay in precise register with the light columns beneath in layer IVc.

Although the functional significance of the cytochrome oxidase patches remains uncertain, they appear to constitute the fundamental cytoarchitectonic unit of primate visual cortex, corresponding to the basic modules postulated by Hubel & Wiesel (1977) on the basis of physiological evidence. Moreover, comparative anatomical studies have indicated that the patches are present only in the striate cortex of primates (Horton 1984). This report describes the successful application of the cytochrome oxidase stain to autopsy specimens of human brain. We find that patches of cytochrome oxidase activity are present in human striate cortex, in common with other primate species. We have also used the cytochrome oxidase technique to demonstrate the presence of ocular dominance columns, confirming Hitchcock & Hickey's original suggestion.

2. Materials and methods

Cytochrome oxidase staining was tested in visual cortex and lateral geniculate nucleus in human autopsy specimens obtained over a period of three years from patients who died from non-neurological causes. Patterns of cytochrome oxidase activity were examined in brains from six adults with normal vision, three adults missing one eye, three infants, and one foetus.

Within 8–34 h *post mortem*, the occipital lobes and lateral geniculate nuclei from each brain were placed in 2% (by volume) glutaraldehyde in 0.1 M phosphate buffer at 4 °C. After about 1 h, the leptomeninges were stripped away and the sulci gently prised open to allow more even penetration of fixative. When the tissue was firm enough for sectioning, usually after 6–10 h, it was removed from fixative, rinsed, and photographed for purposes of orientation and scale. It was then embedded in an albumin–gelatin mixture that hardens rapidly on addition of glutaraldehyde to allow immediate sectioning (Frank *et al.* 1980). To help with the alignment of successive sections, three holes were bored through the block using a 19-gauge needle. The embedded tissue was subsequently frozen by placing it directly on a brass plate cooled to −70 °C by a dry ice–ethanol slurry. Since the tissue was not impregnated with sucrose, rapid freezing was necessary to prevent freezing artefact. Sections were cut at 50 μm on a freezing microtome, mounted on gelatin-coated slides and permitted to air dry.

For cytochrome oxidase histochemistry sections were incubated in a solution containing 50 mg diaminobenzidine, 30 mg cytochrome *c* (type III, Sigma) and 20 mg catalase per 100 ml of 0.1 M phosphate buffer, pH 7.4 (Seligman *et al.* 1968). The reaction usually took 5–15 h, occasionally longer if the tissue was unusually well fixed, or a long period had elapsed between time of death and processing of tissue. Control sections were incubated in the presence of potassium cyanide (65 mg 100 ml^{-1}).

Although the cytochrome oxidase technique generally yields excellent results in unperfused

tissues there are several potential sources of artefact. The enzyme is tightly bound to the inner mitochondrial membrane so diffusion does not occur *post mortem*. However, immersion fixation can produce fictitious patterns of cytochrome oxidase staining, especially if uneven diffusion of fixative occurs into the tissue block. Endogenous peroxidases within erythrocytes can contribute nonspecific background activity. Catalase was always included in the incubation bath to keep H_2O_2 levels low, so that peroxidases were unable to catalyse formation of diaminobenzidine reaction product. Nevertheless, if incubation times were long, resulting in depletion of catalase in the reaction solution, artefactual labelling of red blood cells was often visible.

Acetylcholinesterase activity was made visible by using procedures detailed in Horton (1984). Occasional sections were also stained with cresyl violet.

Cell size measurements in the cortex were performed by drawing cells at $\times 1250$ in a microscope equipped with a camera lucida attachment. Cell areas were then calculated by drawing each cell's outline on a graphics tablet linked to a PDP-11/34 computer. Measurements of ocular dominance column areas were made in a similar fashion by sketching column boundaries on the graphics tablet.

3. Results

(*a*) *Cytochrome oxidase staining in normal human striate cortex*

A coronal section through striate cortex from a normal specimen stained with cresyl violet is illustrated in figure 1*a*, plate 1. The laminar organization of cell bodies closely resembles the plan seen in the macaque monkey although the cortex is distinctly thicker. It is difficult to compare cortical thickness measured in different specimens because conditions of fixation, sectioning, and staining can vary. However, we have made measurements in several human specimens and four unperfused macaque brains processed according to very similar techniques and consistently find a 10–30% greater thickness in man. The laminar pattern in human visual cortex is rather less striking than in macaque visual cortex, perhaps because the cell layers are not so compressed.

An adjacent section stained for cytochrome oxidase (figure 1*b*) showed a thick dark swath running through the middle of the cortex in layer IVc. The lower border appears sharp, in contrast with the relatively light staining in layer V. Above, cytochrome oxidase staining decreases more gradually towards the upper layers. In various species of monkeys a thin 'upper tier' projection from the lateral geniculate nucleus terminates in layer IVa (Hubel & Wiesel 1972; Weber *et al.* 1977; Hendrickson *et al.* 1978). In the macaque, cytochrome oxidase staining in this sublayer is organized into a peculiar 'honeycomb' pattern, corresponding precisely to the arrangement of geniculate afferents (Horton 1984). In the human striate cortex we have been unable to identify a layer IVa in the Nissl stain, nor have we detected a honeycomb pattern of cytochrome oxidase staining between layers IVb and III. Accordingly, we have not designated a layer IVa in figure 1*a*.

In the upper layers there are periodic columns of darker cytochrome oxidase staining spaced about 1 mm apart (figure 1*c*, arrows). They extend from the pia through layers II, III and IVb to the top of layer IVc. In sections cut parallel to the cortical layers these columns are seen as a system of patches, most clearly in layers II, III, and IVb (figure 2*a*, *b*, plate 2) but also in layers V and VI (figure 2*c*). The patches seem to merge directly with the dense band in

layer IVc, unlike in the macaque where the honeycomb and the faint staining of patches in IVb create the appearance of a gap between the patches in supragranular layers and layer IVc. In man the cytochrome oxidase patches are surprisingly well labelled in layer IVb and can be seen faintly even in layer IVc_α. In layer IVc_β no pattern is visible in tangential sections through normal human striate cortex. A pattern of cytochrome oxidase staining is also present in area 18 and other unidentified extrastriate visual areas (figure 2).

To get a clearer idea of the pattern formed by the patches in layers II and III a montage was prepared by glueing together portions of photographs of consecutive sections cut tangentially through the occipital lobe in a third case (figure 3, plate 3). The patches were varied in shape, sometimes round but usually oval, measuring about 250–400 μm with a density of one patch per 0.6–0.8 mm^2 of cortex. These estimates are imprecise because the patches are rather irregular and poorly demarcated. In portions of figure 3 the patches appear organized into rows intersecting the 17–18 border at right angles. This is seen more clearly in a tangential section through the upper layers from another normal case (figure 4). Along some rows the patches are confluent, forming long beaded strips. Each row of patches ends abruptly at the 17–18 border; the spacing between adjacent rows is about 1 mm, along each row a patch is located about every 0.75 mm.

In one normal human specimen alternate sections were processed for cytochrome oxidase and AChE activity to compare distributions of the two enzymes. In layer II, III the AChE stain showed faint patches (figure 5*a*) that matched the patches labelled by cytochrome oxidase in a section from the same block (figure 5*b*). In the light microscope AChE activity appeared to be located mainly in fibres, synaptic processes, and on the surface of cell bodies. Relatively few cell bodies showed high enzyme content in striate cortex, although in area 18 a tier of diffusely labelled cells was present in layer IV.

(*b*) *Effect of eye removal on cytochrome oxidase staining in human lateral geniculate nucleus*

Wong-Riley (1979) has reported loss of cytochrome oxidase activity in denervated laminae of the geniculate following eye removal in the cat. We tested cytochrome oxidase activity in the lateral geniculate nucleus in two patients who died many years after losing one eye as adults. Similar findings were obtained in the two cases. Figure 6, plate 4 shows a section through the left and right geniculate bodies of a 57 year old man whose left eye was removed following a retinal haemorrhage 23 years earlier. Cresyl violet stained sections through the right (figure 6*a*) and left (figure 6*b*) geniculates showed the classical pattern of anterograde transneuronal degeneration first described by Minkowski (1920) after eye removal in the rhesus monkey. Ipsilateral to the missing eye, laminae 2, 3 and 5 appear pale and atrophied; the same is true contralaterally for laminae 1, 4 and 6.

A higher power view straddling laminae 6 and 5 from figure 6*b* is shown in figure 7*a*, plate 5. Above, the normally innervated lamina 6 is separated by fibres in the relatively cell-sparse interlaminar zone from the denervated lamina 5 below. If the appearance of cells in the two laminae are compared, severe atrophy of neurons is evident in lamina 5; indeed it is hard to distinguish them from glia.

Closely adjacent sections stained for cytochrome oxidase show a striking loss of enzyme activity in denervated parvocellular laminae. If each pair of sections are compared (figures 6*a*, *c*; 6*b*, *d*) the same set of laminae appear pale in both cytochrome oxidase and Nissl stains. Unfortunately, excessive fixation destroyed cytochrome oxidase activity in normal and

denervated magnocellular laminae bilaterally. At higher power (figure 7*b*), the same region of geniculate illustrated in figure 7*a* is shown stained for cytochrome oxidase. In lamina 6 intense enzyme activity is evident in diffusely labelled principal cells. In addition, there is abundant staining in the neuropil, probably located in dendrites of principal cells and axon terminals of retinal ganglion cells and layer VI cortical neurons. In denervated lamina 5 cytochrome oxidase activity is much weaker. Shrunken cell bodies are faintly delineated against a pale background of enzyme staining. These results indicate that cellular atrophy, as demonstrated by Nissl staining following enucleation, is accompanied by a profound drop in levels of metabolic enzymes. This effect is not restricted to cytochrome oxidase. Loss of NADH diaphorase, isocitrate, glutamate and lactate dehydrogenase has been observed in the monkey geniculate body following removal of one eye (Gay & Silberberg 1964; Cotlier *et al.* 1965).

(*c*) *Effect of eye removal upon cytochrome oxidase staining in human striate cortex*

In this section material will be presented primarily from the case described in the previous section, a 57 year old man who died 23 years after removal of the left eye. The effects of monocular enucleation upon the geniculate body were illustrated in figures 6 and 7.

Description of plates 2, 3 and 4

Figure 2. A series of parasagittal sections cut tangential to the medial face of the left occipital lobe from a 64 year old man. Brain was obtained 9 h *post mortem* and fixed for 7 h in 2% (by volume) glutaraldehyde. Tissue was incubated in cytochrome oxidase reaction solution for 8 h.

(*a*) The calcarine and parietooccipital fissures are indicated by large arrows, superior is up and anterior to the right. The border between area 17 and area 18 is marked by a series of small arrows. In layers II and III a system of small cytochrome oxidase patches is obvious.

(*b*) In deeper portions of cortex the patches appear to merge into layer IV as labelling increases in intensity. No pattern can be discerned in layer IVc_β although a hint of patches is sometimes noticed in IVc_α.

(*c*) Infragranular layers also contain patches, more weakly staining but located in perfect register with the patches in II, III. Thus each patch is actually a pillar, extending from layer I to VI, interrupted only in IVc_β. Notice irregular pattern of cytochrome oxidase staining in extrastriate cortex, and lack of cytochrome oxidase activity in white matter (w) which is visible in deeper regions of sections in (*b*) and (*c*). Scale = 5 mm.

Figure 3. A montage of photographs from sections cut tangential to the medial face of the left occipital lobe from another normal human brain. The cytochrome oxidase stain in layers II and III reveals an irregular array of patches, spaced about one patch per 0.6–0.8 mm^2. The 17–18 border is indicated by arrows; in some regions the patches appear aligned in rows approaching perpendicular to the 17–18 boundary. In area 18 a pattern of cytochrome oxidase staining is also visible. Scale = 2 mm.

Figure 4. Single tangential section through occipital lobe from another normal specimen. The 17–18 border running along superior and inferior banks of calcarine fissure is marked by large arrows. Six small arrows spaced about every 1 mm indicate rows of patches oriented at right angles to striate cortex boundary. Confluence of patches along each row is apparent. Where the section grazes the top of layer IVc enzyme staining appears darkest and the pattern of patches is obscured. Scale = 2 mm.

Figure 5. Comparison of cytochrome oxidase and AChE staining in normal human striate cortex.

(*a*) Section stained for AChE shows a very faint pattern of patches in layers II and III; more intense enzyme activity represents layer IV.

(*b*) A second 250 μm more superficial from the same block of tissue stained for cytochrome oxidase shows a clear pattern of patches. Careful comparison of (*a*) and (*b*) has confirmed that labelled patches visible in both sections coincide in position; three examples of matching patches are indicated by small arrows. Scale = 1 mm.

Figure 6. (*a*) Right and (*b*) left lateral geniculate bodies stained with cresyl violet from a 57 year old man who died 23 years after losing his left eye. Classical pattern of anterograde transneuronal degeneration is visible in laminae 1, 4, and 6 contralaterally and 2, 3, 5 ipsilaterally. (*c*) and (*d*) are closely adjacent sections stained for cytochrome oxidase. Dorsal laminae that appear atrophied in Nissl stain also show severe loss of cytochrome oxidase activity. Pale appearance of ventral layers is because of destruction of cytochrome oxidase reactivity by overexposure to glutaraldehyde up to the boundary of fixative penetration passing between pairs of curved arrows. Scale = 1 mm.

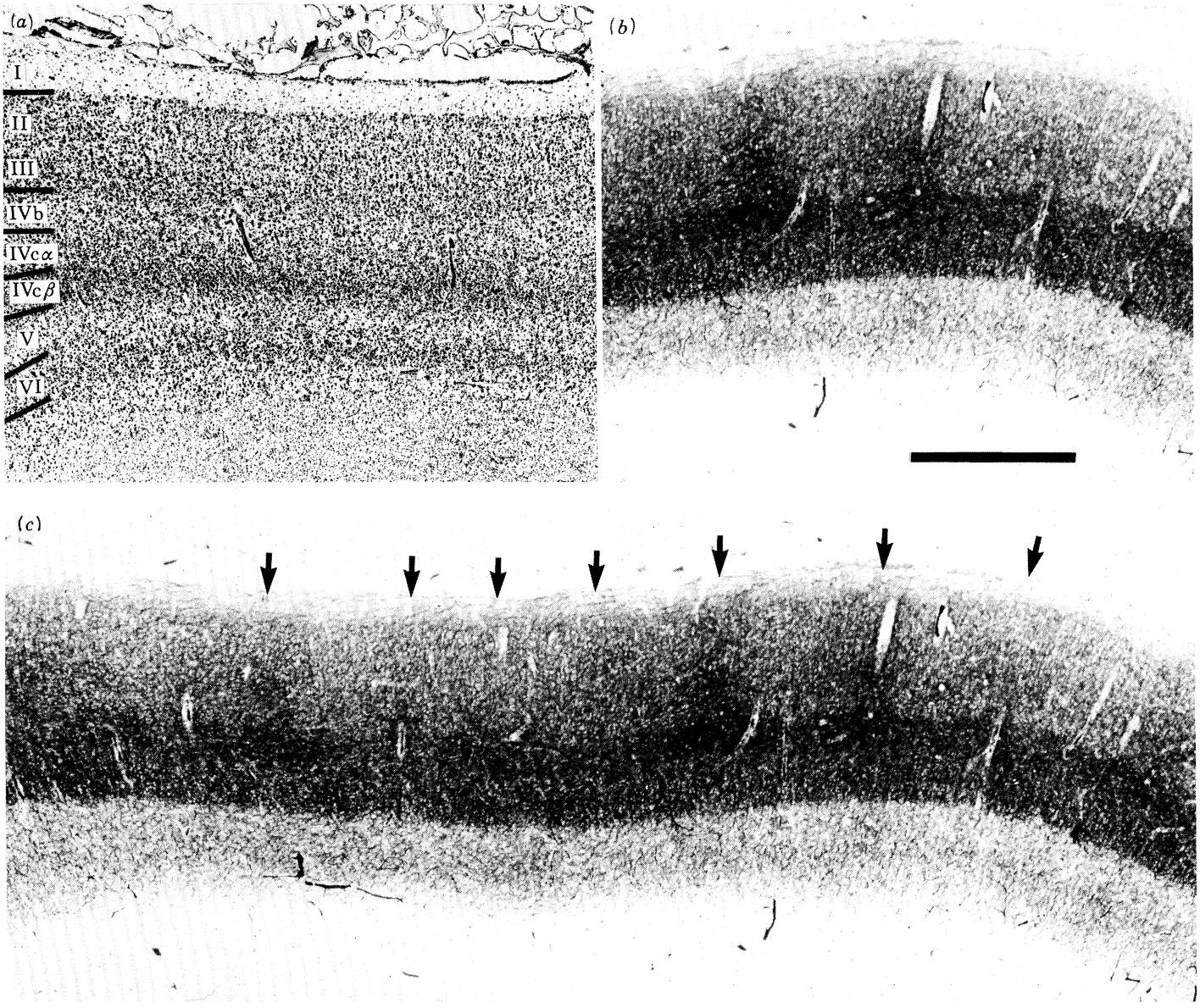

FIGURE 1. Coronal sections through normal human striate cortex (primary visual cortex, area 17) obtained *post mortem*.

(*a*) Cresyl violet stain shows classical appearance of the layers, with a densely cellular layer IVc and a relatively cell-sparse layer IVb above containing the stria of Gennari.

(*b*) An adjacent section stained for cytochrome oxidase shows a dense band in layer IVc, sharing a sharp lower border with layer V that stains more weakly. Note the absence of an 'upper tier' of intense cytochrome oxidase activity characteristic of layer IVa in a macaque. Staining is also surprisingly rich in layer IVb.

(*c*) In the cytochrome oxidase stain periodic vertical columns of enhanced enzyme activity are visible in the upper layers, spaced about 1 mm apart (arrows). Scale = 1 mm.

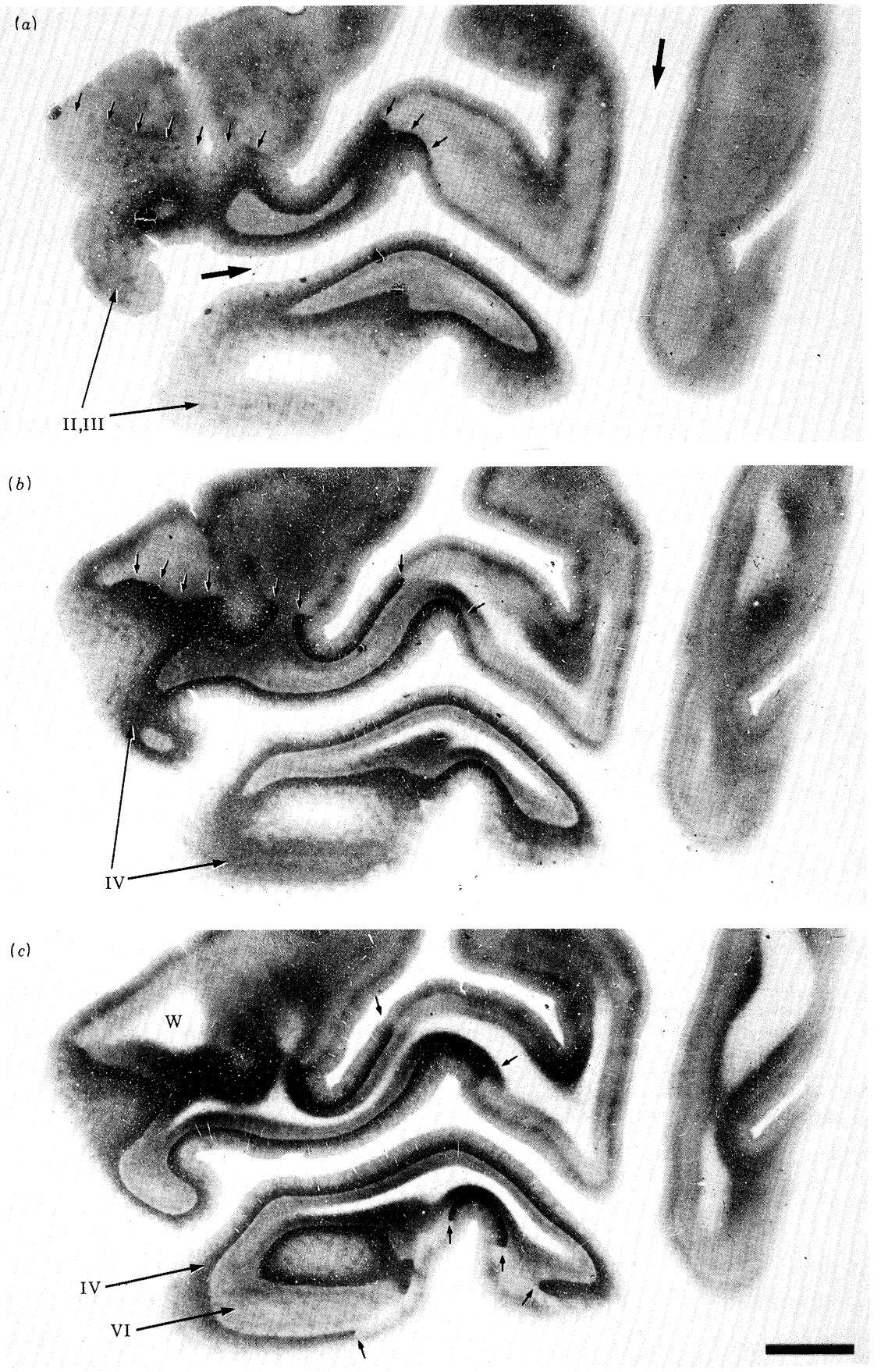

FIGURE 2. For description see p. 260.

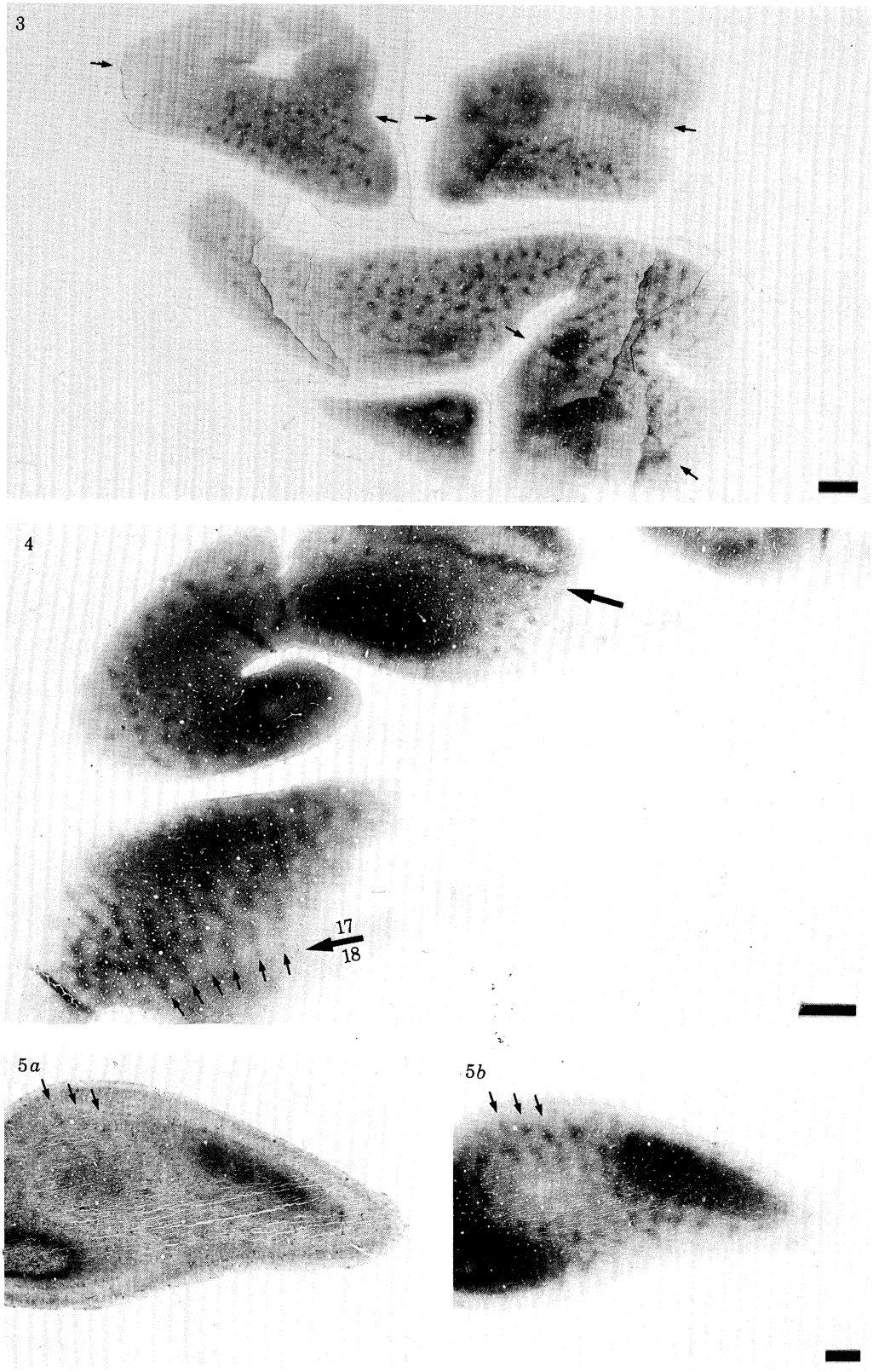

FIGURES 3–5. For description see p. 260.

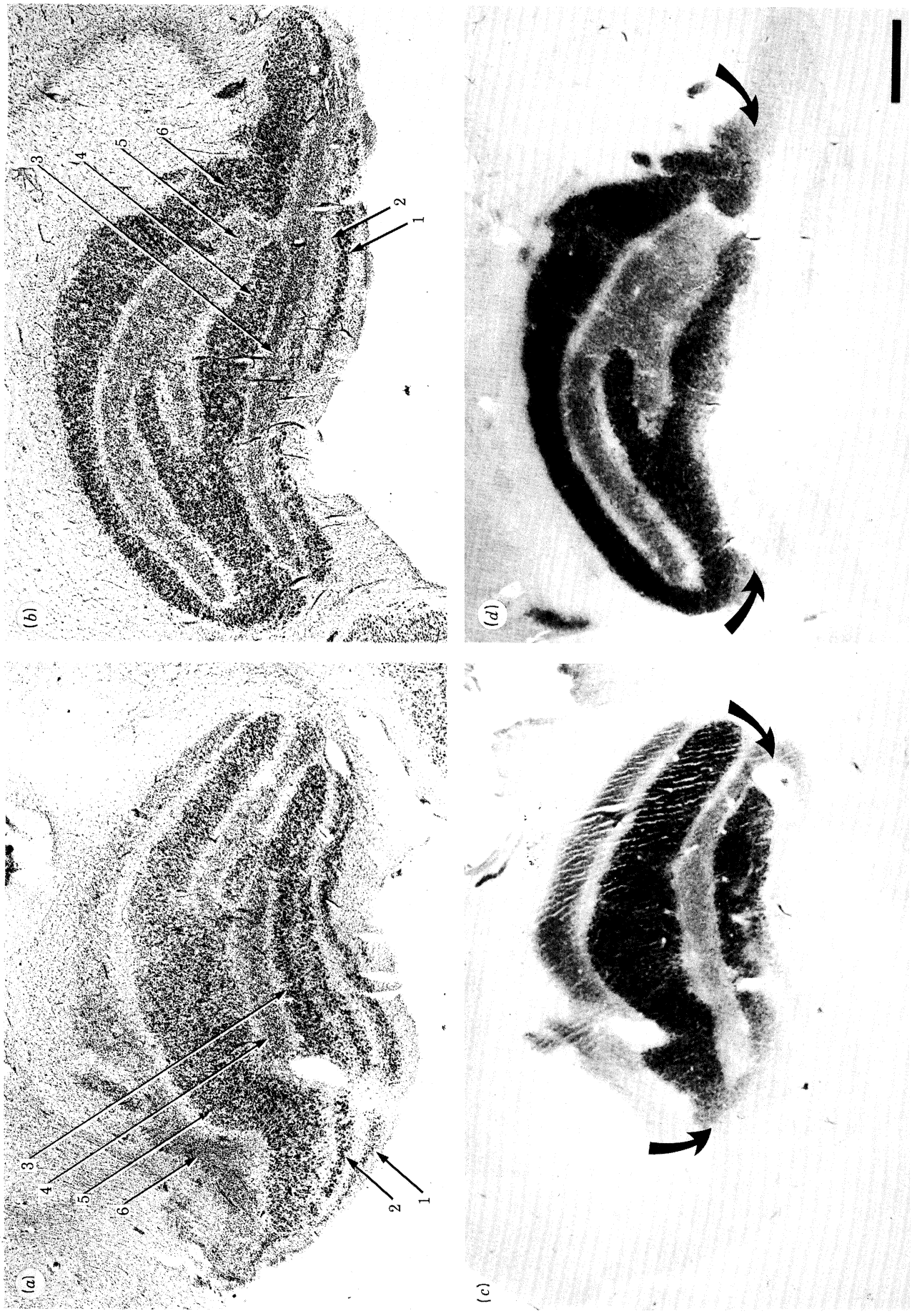

FIGURE 6. For description see p. 260.

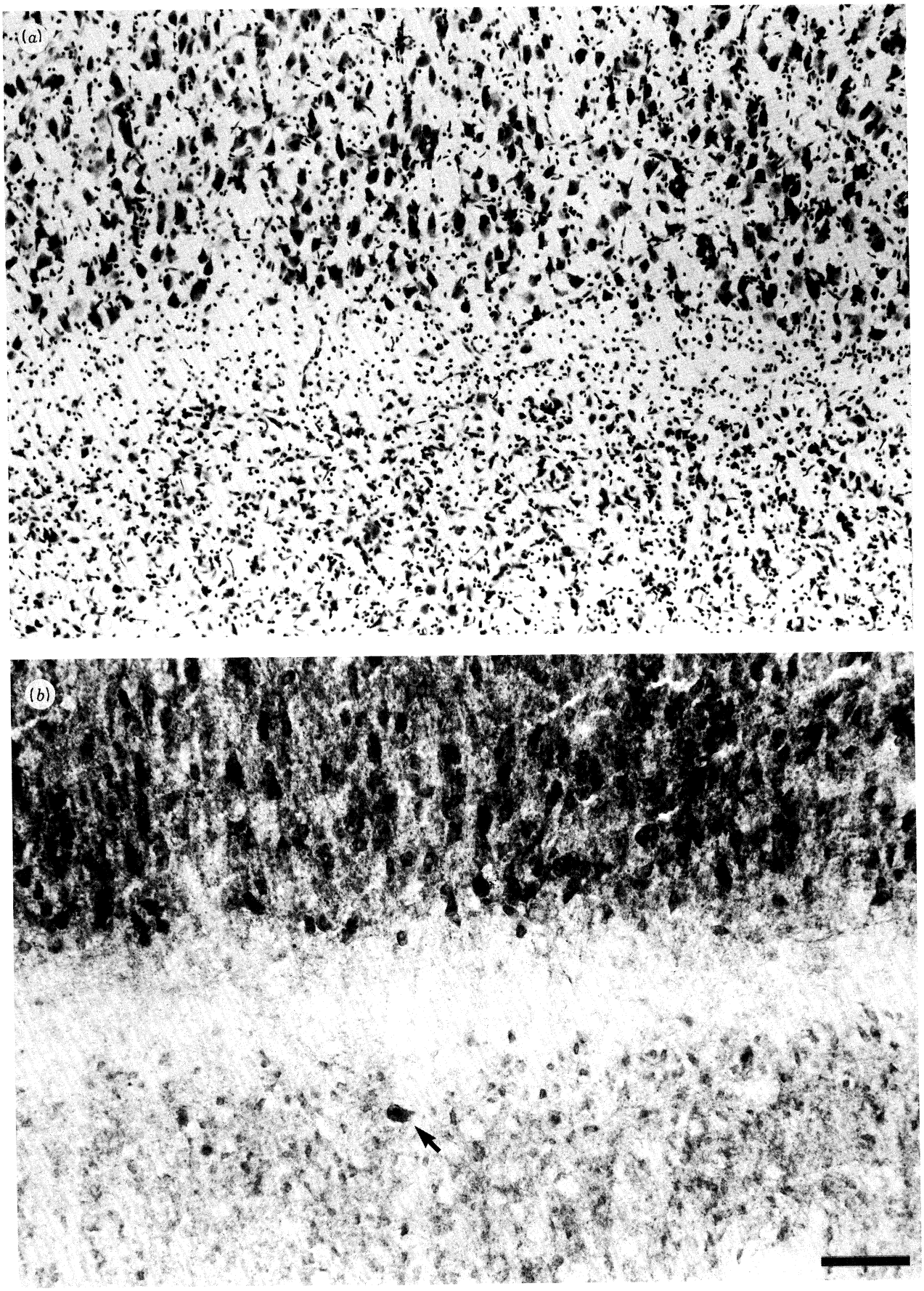

FIGURE 7. For description see p. 261.

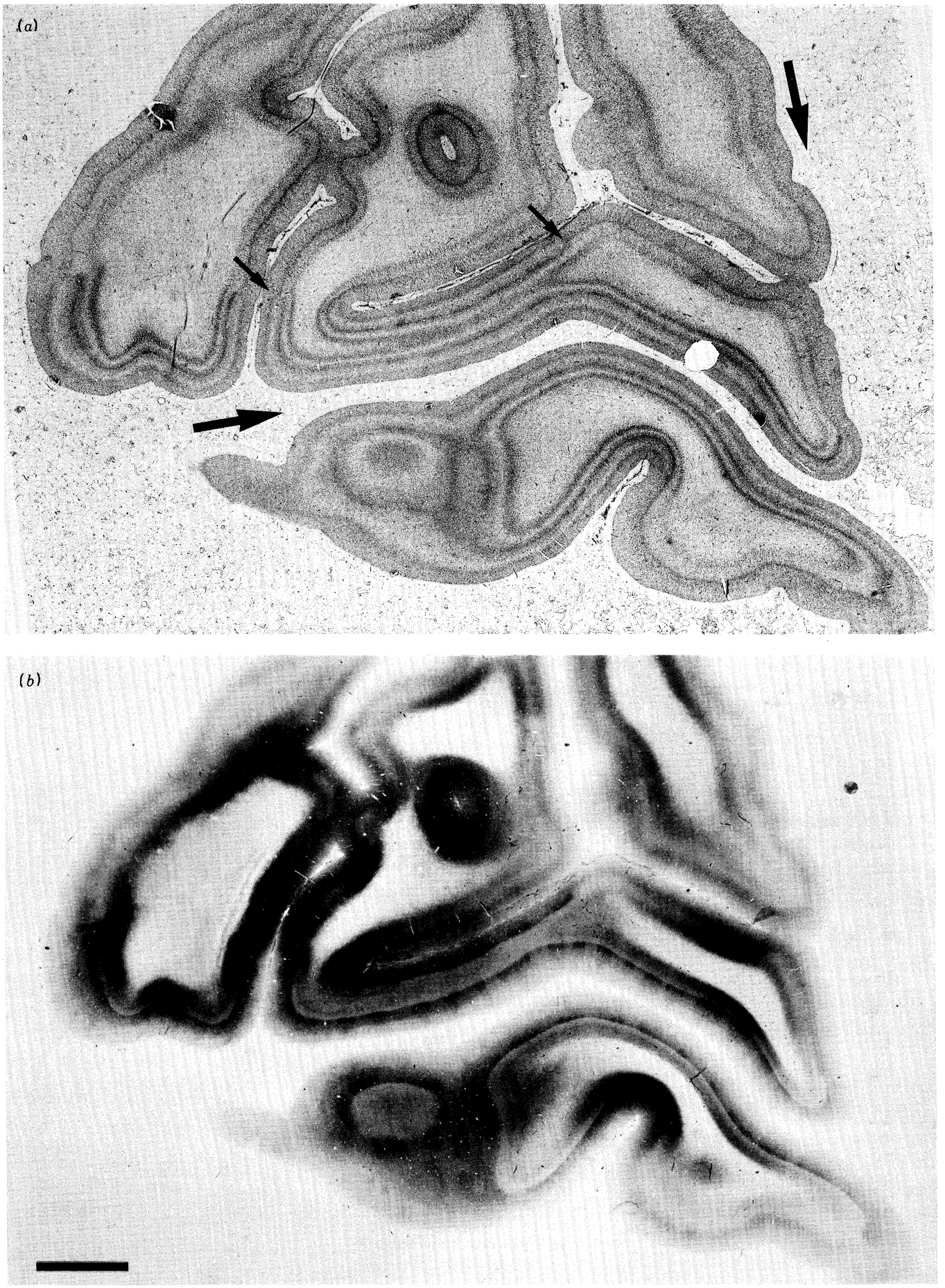

FIGURE 8. For description see p. 261.

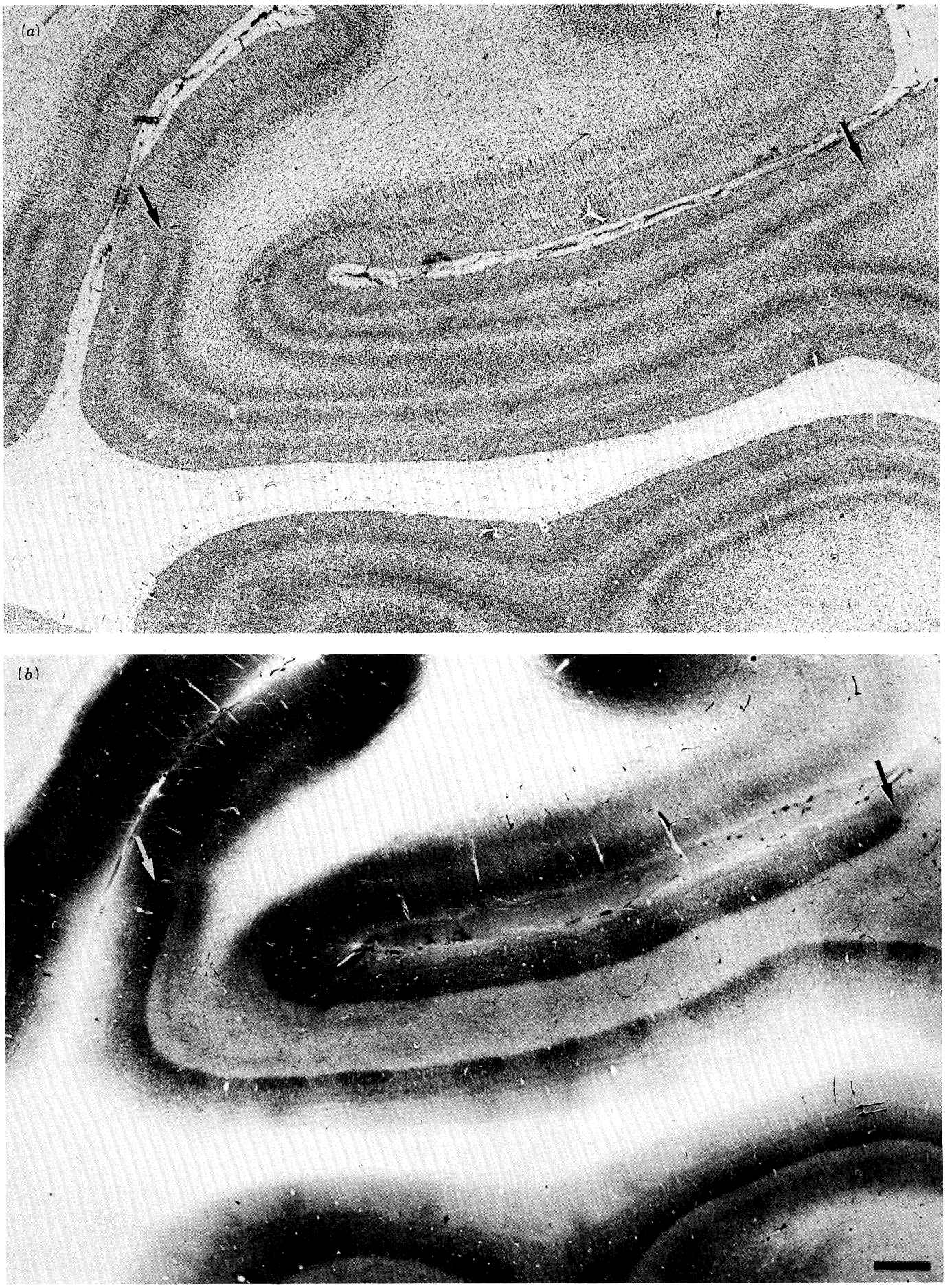

FIGURE 9. For description see p. 261.

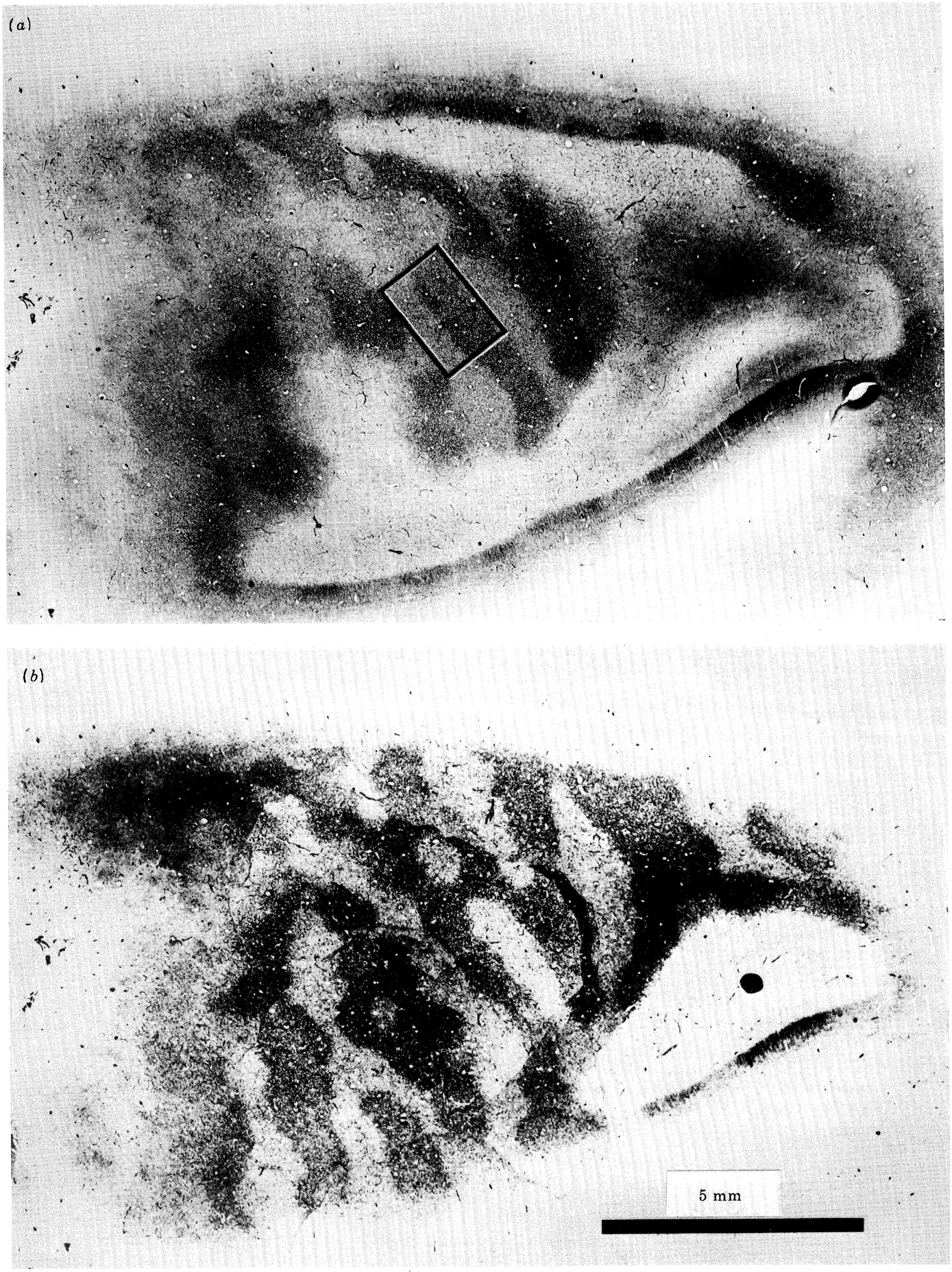

FIGURE 10. For description see opposite.

(i) *Appearance of ocular dominance columns in layer IV*

Figure 8*a*, plate 6 shows a Nissl-stained parasagittal section cut tangentially to the medial face of the left occipital lobe. The overall orientation of the block is exactly the same as for the normal case shown in figure 2. Striate cortex is visible along the banks of the calcarine fissure; in a few places we have marked the 17–18 border with small arrows. An adjacent section (figure 8*b*) stained for cytochrome oxidase reveals a striking abnormality: a regular pattern of alternating light and dark columns about 1 mm wide visible in layer IV. In normal striate cortex (figure 2), layer IVc shows no hint of such a pattern. In the macaque monkey a similar pattern of light and dark columns is also seen after eye removal. Correlation with 2-deoxyglucose radioautography and [^{3}H]proline transneuronal radioautography has established that in the monkey the cytochrome oxidase pattern corresponds to the ocular dominance columns, and that darkly staining columns belong to the remaining eye (Horton 1984). While direct evidence is lacking in a man, we assume the pattern visible in figure 8*b* represents the ocular dominance columns in human striate cortex.

Description of plates 5–8

FIGURE 7. (*a*) Higher power view from figure 6*b*. Normal cells in lamina 6 (upper half) are separated by the fibre rich interlaminar zone from denervated cells in lamina 5 (lower half). In lamina 5 severe atrophy of principal cells is obvious in Nissl stain.

(*b*) Same region as in (*a*), stained for cytochrome oxidase. In lamina 6 each geniculate principal cell is intensely labelled by cytochrome oxidase. In addition, considerable cytochrome oxidase activity is visible in the neuropil, probably located in axon terminals of retinal ganglion cells, in axon terminals of cortical layer VI cells, and in dendritic processes of geniculate principal cells. In lamina 5, atrophied geniculate neurons appear shrunken and stain weakly for cytochrome oxidase. Background staining in the neuropil is also drastically reduced. Rare isolated cells (arrow) appear quite normal. Scale = 100 μm.

FIGURE 8. (*a*) Parasagittal section cut parallel to the medial face of the left occipital lobe from the case illustrated in figure 6. Orientation is similar to the section shown in figure 2 from a normal case. The large horizontal arrow indicates the calcarine sulcus and points anteriorly. The large vertical arrow marks the parieto-occipital sulcus and points inferiorly; brain anterior to the parietooccipital sulcus was trimmed from the block before embedding. In the cresyl violet stain striate cortex is seen along the banks of the calcarine sulcus; the 17–18 border is marked by small arrows in two locations; six other junctions between straite and extrastriate cortex can be readily identified but have not been marked by arrows.

(*b*) An adjacent section stained for cytochrome oxidase activity. The brain was obtained at autopsy 17.5 h after death. After immersion fixation of the occipital lobe in 2% (by volume) glutaraldehyde for 6 h the tissue was cut and reacted for 13 h. In striate cortex a regular pattern of alternating light and dark columns about 1 mm wide is visible in layer IV. These columns, which are absent in normal striate cortex, presumably represent the ocular dominance columns in human visual cortex. Scale = 5 mm.

FIGURE 9. (*a*) Region from figure 8*a* seen at higher magnification. The two arrows, whose tips abut layer IV, match the pair of arrows in figure 8*a*. In layer IV a regular fluctuation in the density of staining is apparent. Darker areas, which match the light columns of cytochrome oxidase staining in (*b*), correspond to regions of more densely packed, atrophied cell bodies. This effect is also seen faintly in cortex above layer IV.

(*b*) Matching area from figure 8*b* shown at the same scale. Two large arrows again indicate the 17–18 frontiers. Note pattern of ocular dominance columns in layer IV, most clearly demarcated in IVc. The patches in layers II and III are faded over pale staining ocular dominance columns in layer IV. In layer IVb two faint, thin stripes of darker cytochrome oxidase activity are apparent (small arrows); their significance is unknown. Scale = 1 mm.

FIGURE 10. (*a*) Tangential section grazing layer IV from right striate cortex of the same case illustrated in figures 8 and 9. In layer IVc the ocular dominance columns are viewed *en face*, appearing as light and dark parallel slabs. Elsewhere they are cut in cross-section and appear as alternating light and dark columns. To the left the patches are visible in layer III, in layer V cytochrome oxidase staining appears very pale. Area enclosed in black box is shown in figure 13*b*.

(*b*) Montage of layer IVc prepared by glueing together portions of photographs from 12 serial sections stained for cytochrome oxidase, including the section shown in (*a*). The ocular dominance columns are irregular in width, show frequent bifurcations, blind endings, and islands. The increased contrast between light and dark columns compared with (*a*) is an artefact produced by rephotographing the montage.

A region from figure 8 viewed at higher power is shown in figure 9, plate 7. In the Nissl stain (figure 9*a*) layer IV has a mottled appearance, showing a periodic waxing and waning in density of cell bodies. By referring to an adjacent section (figure 9*b*) stained for cytochrome oxidase, we have verified that this pattern bears a close relation with the ocular dominance columns in IVc. Each small zone in layer IV that appears slightly darker in cresyl violet matches exactly an ocular dominance column that stains more lightly for cytochrome oxidase. This finding will be taken up again in more detail in a later section.

In figure 9*b* the ocular dominance columns appear more distinct in layer IV c_β than in IV c_α, as in the macaque. Their borders are quite sharp, especially compared with the rather gradual fluctuations in staining seen in the Nissl. Above the light columns in layer IV the patches in layers II and III appear paler than their counterparts situated over normal eye columns. In layer IVb two thin parallel stripes of enhanced cytochrome oxidase activity are visible. In some normal brains we have noted a single, but never a pair, of stripes in layer IVb. In the macaque, an extra band of cytochrome oxidase develops at the base of layer IV following enucleation; two extra bands are induced by eyelid suture. We are not sure if the two parallel stripes seen in the human are a consequence of eye removal, or if we have simply failed to detect them in our normal material. In the light microscope they do not resemble the honeycomb layer seen in IVa of the macaque.

For a clearer impression of the pattern formed by the ocular dominance columns it is best to view them in tangential, rather than coronal, section. Figure 10*a*, plate 8 shows a small portion of a tangential section grazing layer IV from the right striate cortex of the same brain illustrated in figures 8 and 9. Within layer IV the ocular dominance columns are visible; elsewhere the section passes into layer III and layer V. A montage, prepared in the same manner as figure 3, shows the pattern of ocular dominance columns over a wider area (figure 10*b*) in layer IV. The columns viewed *en face* appear as alternating light and dark parallel slabs, irregular in width, with frequent blind endings and lacunae.

(ii) *Effect of eye removal on the cytochrome oxidase patches*

A section through the upper layers (figure 11*a*, plate 9) shows the patches from the same block of tissue illustrated in figure 10. The patches are quite unevenly stained; some appear smaller and paler, whereas others are darker and more confluent. To determine if these irregularities might be associated with the ocular dominance columns in layer IVc, a reconstruction was prepared (figure 11*b*) by superimposing the borders of the ocular dominance columns in figure 10*b* onto figure 11*a*. It is apparent that the patches follow the pattern of the ocular dominance columns and that patches lying within the borders of dark ocular dominance columns belonging to the intact eye show stronger cytochrome oxidase staining. This is true not only for the patches, but also for cortex immediately surrounding them situated within the confines of the dark column boundaries. The patches located within enucleate-eye columns stain more weakly, although they are still readily visible even 23 years after loss of the eye. This pattern of alternating light and dark patches in register with light and dark ocular dominance columns in IVc was also apparent in coronal sections through the cortex (figure 9*b*).

(iii) *Secondary transneuronal anterograde degeneration in the cortex*

Haseltine *et al.* (1979) have reported the development of secondary transneuronal anterograde degeneration in striate cortex of a macaque monkey 29 months after monocular enucleation.

Regions of alternating light and dark staining were observed in Nissl stained sections through layer IVc, corresponding to the ocular dominance columns. Measurements revealed that cells within dark Nissl columns were 20–30% more densely packed and 7–14% smaller in area than cells in light columns. This result has been confirmed in the macaque, six months after eye removal (Horton 1984).

In the human striate cortex degenerative changes are also visible after monocular enucleation. In a tangential section passing through layer IVc stained with cresyl violet (figure 12*a*, plate 10) faint irregularities in the density of the Nissl stain are seen. The regions appearing

TABLE 1. DIFFERENCE IN SIZE AND DENSITY BETWEEN CELLS IN NORMAL AND ENUCLEATE EYE COLUMNS†

	normal eye dominance columns		enucleate eye dominance columns	
	neurons	glia	neurons	glia
average area	57.3 μm²	25.2 μm²	51.9 μm²‡	26.8 μm²§
n	191	174	257	268
σ_n	18.7	9.60	13.1	10.1
s.e.m.	1.35	0.73	0.82	0.62

† For measurements of cell density and size every cell in three pairs of microscope fields (at × 1250:0.0176 mm² per field of view) was drawn and counted. Each pair of microscope fields fell on either side of the boundary between two adjacent columns in layer IVc, one field in a normal eye column and one field in an enucleate eye column. One pair of microscope fields was analysed in the area shown in figure 13*a*.

‡ Significantly smaller than neurons in normal eye columns ($p < 0.02$, two-tailed Student's t-test).

§ Not significantly different from glia in normal eye columns ($p > 0.10$, two-tailed Student's t-test).

slightly darker are indicated schematically with small black dots in figure 12*b*. Borders of the ocular dominance columns are drawn from an adjacent cytochrome oxidase stained section (figure 10*a*) and columns belonging to the intact eye are filled in with parallel diagonal lines. When referring to the reconstruction it is apparent that the set of ocular dominance columns that stains more darkly with cresyl violet matches the set of columns exhibiting weaker cytochrome oxidase activity, corresponding to the missing eye.

At higher power (figure 13*a*, plate 11) cells in the darker Nissl-stained columns appear slightly shrunken and more densely packed than cells in the light columns. To test this impression, quantitative measurements of cell area and number were made in layer IVc for neurons and glia in normal and enucleate eye columns (table 1). In enucleate-eye columns, neuronal somata were shrunken by about 10% in cross-sectional area, equivalent to a 15% volume loss, and packed 35% more tightly. These results are in good agreement with those of Haseltine *et al.* (1979). No significant change in size of glia was found, but their density is also increased in enucleated-eye columns, by 54%. Although our measurements were limited to layer IVc, degeneration was also noticed occasionally in layers III and II, in areas above enucleate-eye columns in IVc (figure 9*a*).

The same region from an adjacent section reacted for cytochrome oxidase is shown in figure 13*b*. Enzyme activity is weaker in the ocular dominance column that stains more darkly with cresyl violet. Note also the fine reticular pattern formed by the cytochrome oxidase stain visible in both the light and dark ocular dominance columns in layer IVc. Most of the enzyme label is present in the neuropil rather than in stellate cell bodies, but outside IVc diffusely labelled neurons are commonly seen.

(iv) *Pattern formed by ocular dominance columns in human striate cortex*

The pattern formed by ocular dominance columns in the macaque over the posterior opercular convexity (central 8° of visual field) has been reconstructed by LeVay *et al.* (1975). We attempted to reconstruct as much as possible of the column pattern in the human to see how it might compare with the macaque. In figure 10*b* a partial reconstruction was made by glueing together portions of photographs of serial sections. It proved easier to place each slide in a microscope projector to sketch the pattern directly on a large sheet of tracing paper. Figure 14 shows a more complete reconstruction from the hemisphere illustrated in figure 10*b*; the area shown in the photomontage can be recognized in the lower right. The reconstruction was then superimposed photographically back onto a picture of the gross brain specimen taken just before embedding (figure 15*a*, plate 12). A reconstruction of the opposite hemisphere is shown in figure 15*b*. In the second case examined, a 75 year old woman who lost her left eye ten years previously, we also prepared reconstructions of the columns in both hemispheres (figures 16*a*, *b*, plate 13); only casual observations of the column pattern were made in the third case. When looking at the four reconstructions, the ocular dominance columns appear quite irregular, frequently anastomosing and bifurcating with numerous blind loops and small

Description of plates 9–11

Figure 11. (*a*) Tangential section cut 550 μm superficial to the section illustrated in figure 10*a*. The cytochrome oxidase patches are obvious in layer III, and even visible to the right in layer IVb. No montage is necessary because layers II and III are thicker than layer IVc, allowing patterns to be seen over a wider area in a single section. The patches appear irregularly stained, showing a branching pattern of lighter and darker segments.

(*b*) Same section as in (*a*), rephotographed with the pattern of ocular dominance columns in layer IVc superimposed. Reconstruction was prepared by tracing the ocular dominance columns in figure 10*b* onto a clear acetate sheet. In addition the position of many small blood vessels in the section was marked. Most vessels pass radially through the cortex with little shift in position and can be easily recognized in more superficial sections. By matching the blood vessels in figures 10*b* and 11*a* it was possible to position accurately the acetate sheet with the sketch of ocular dominance columns. It was then rephotographed to produce the reconstruction. Within ocular dominance columns belonging to the intact eye, cytochrome oxidase staining is darker and the patches are more strongly labelled. The opposite is true in columns corresponding to the enucleated eye.

Figure 12. (*a*) Cresyl violet stained section adjacent to cytochrome oxidase stained section of figure 10*a*. Where the section passes through layer IVc the density of the Nissl stain is irregular because of secondary anterograde transneuronal degeneration of cells induced by eye removal. Region enclosed in box, matching box in figure 11*a*, is shown at higher power in figure 13*a*.

(*b*) Schematic reconstruction comparing patterns of ocular dominance columns labelled by cresyl violet and cytochrome oxidase. Small dots indicate more dense Nissl-stained regions from layer IVc in (*a*). The borders of the ocular dominance columns were traced from an adjacent section (figure 10*a*) and the dark cytochrome oxidase stained columns filled in with parallel diagonal lines. For orientation, the tip of the black arrow would touch the left uppermost corner of the box in (*a*). From the reconstruction it is evident that ocular dominance columns that stain more darkly with cresyl violet, corresponding to the enucleated eye, match the set of columns staining more lightly for cytochrome oxidase activity. Scale = 5 mm.

Figure 13. (*a*) Region within black box in figure 12*a* at higher magnification. Boundary separating a normal and an enucleated eye dominance column passes horizontally through the figure, between the two large arrows. Above, within a deprived eye dominance column, neurons appear more densely packed and slightly atrophied. As a result, the column appears darker in the Nissl stain. Curved arrows mark four prominent blood vessels.

(*b*) A matching region from the area enclosed with the box in figure 10*a*; curved arrows mark the same four blood vessels as in (*a*). Again, the frontier between the two ocular dominance columns passes between large arrows. Below, in a column driven by the intact eye, cytochrome oxidase activity is more intense. Comparing (*a*) and (*b*) the conclusion reached from figure 12 is confirmed: darker Nissl columns stain more lightly for cytochrome oxidase. Notice that cytochrome oxidase stain in IVc forms a reticular pattern, similar to the pattern in layer IVc of the monkey, but coarser. The labelling of red blood cells is caused by endogenous peroxidases that also catalyse formation of diaminobenzidine reaction product. Scale = 100 μm.

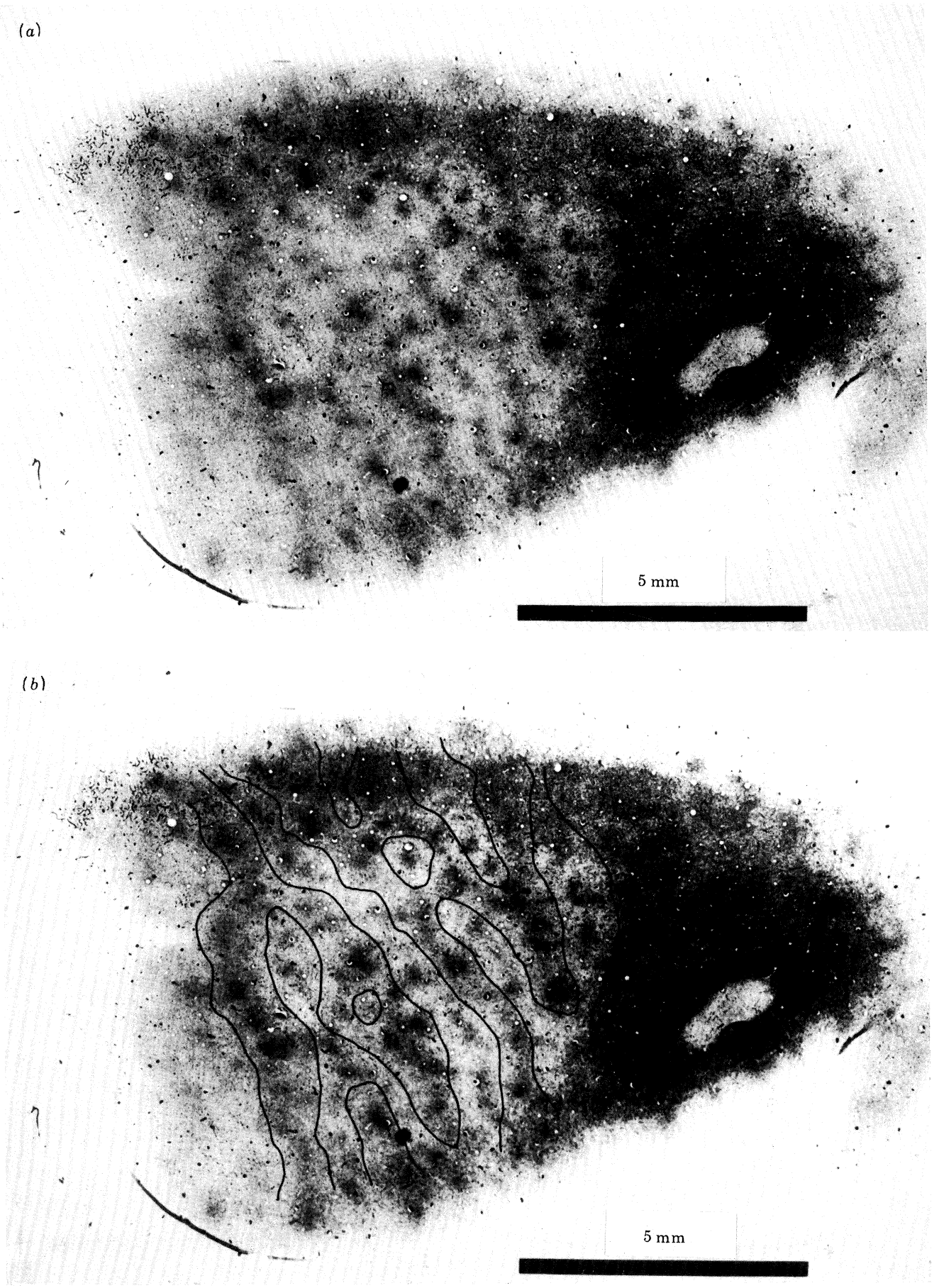

FIGURE 11. For description see opposite.

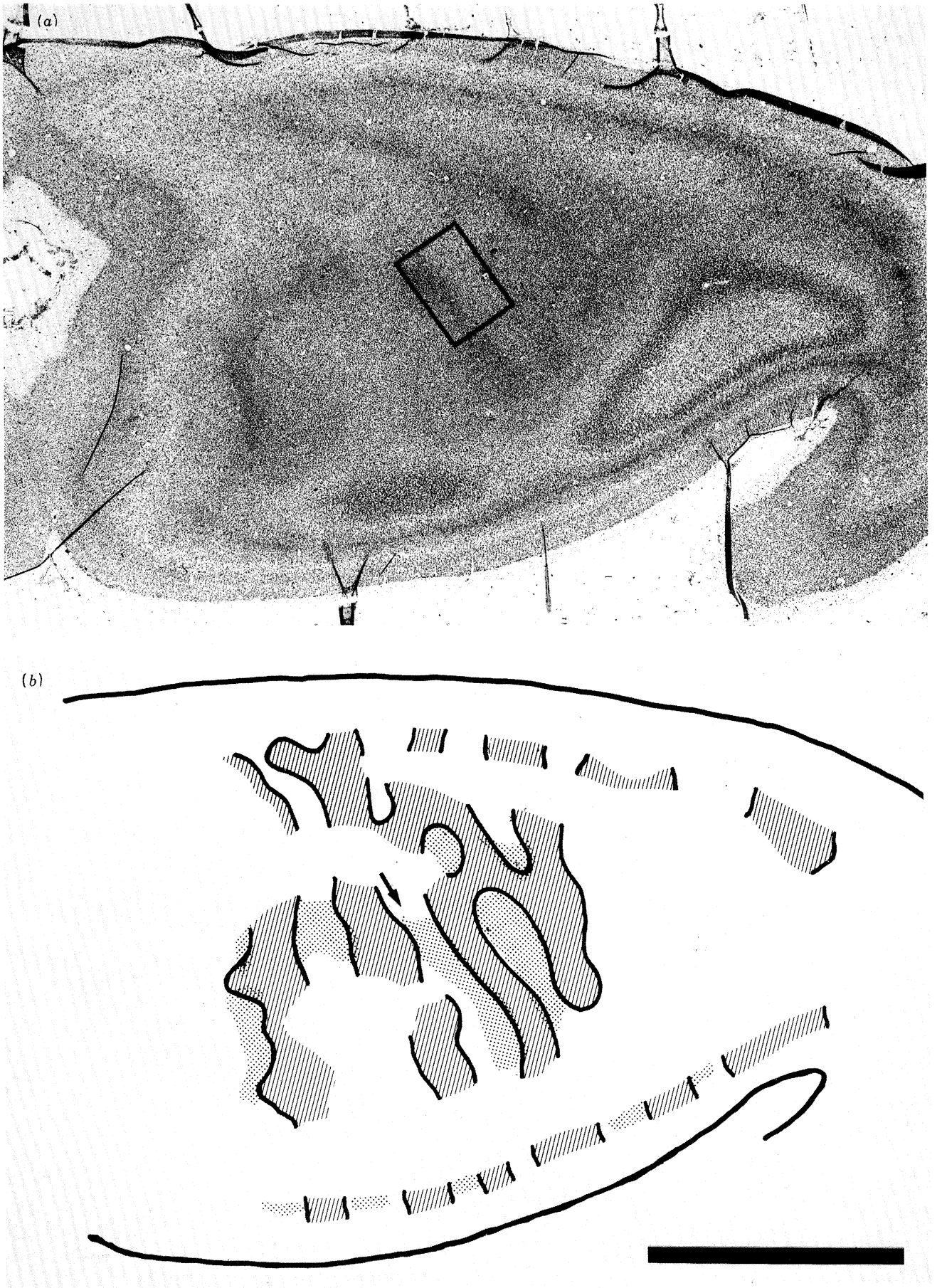

FIGURE 12. For description see p. 264.

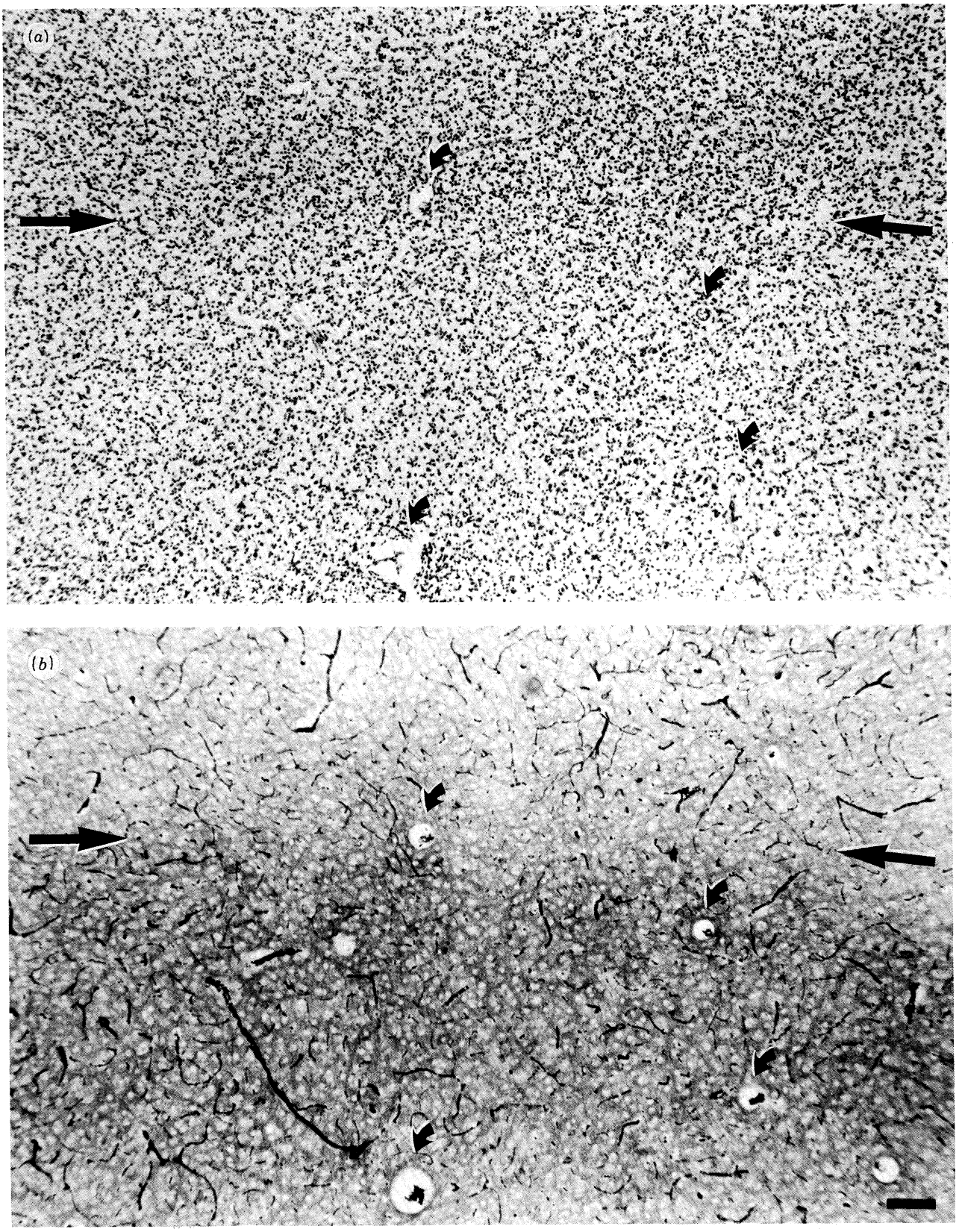

FIGURE 13. For description see p. 264.

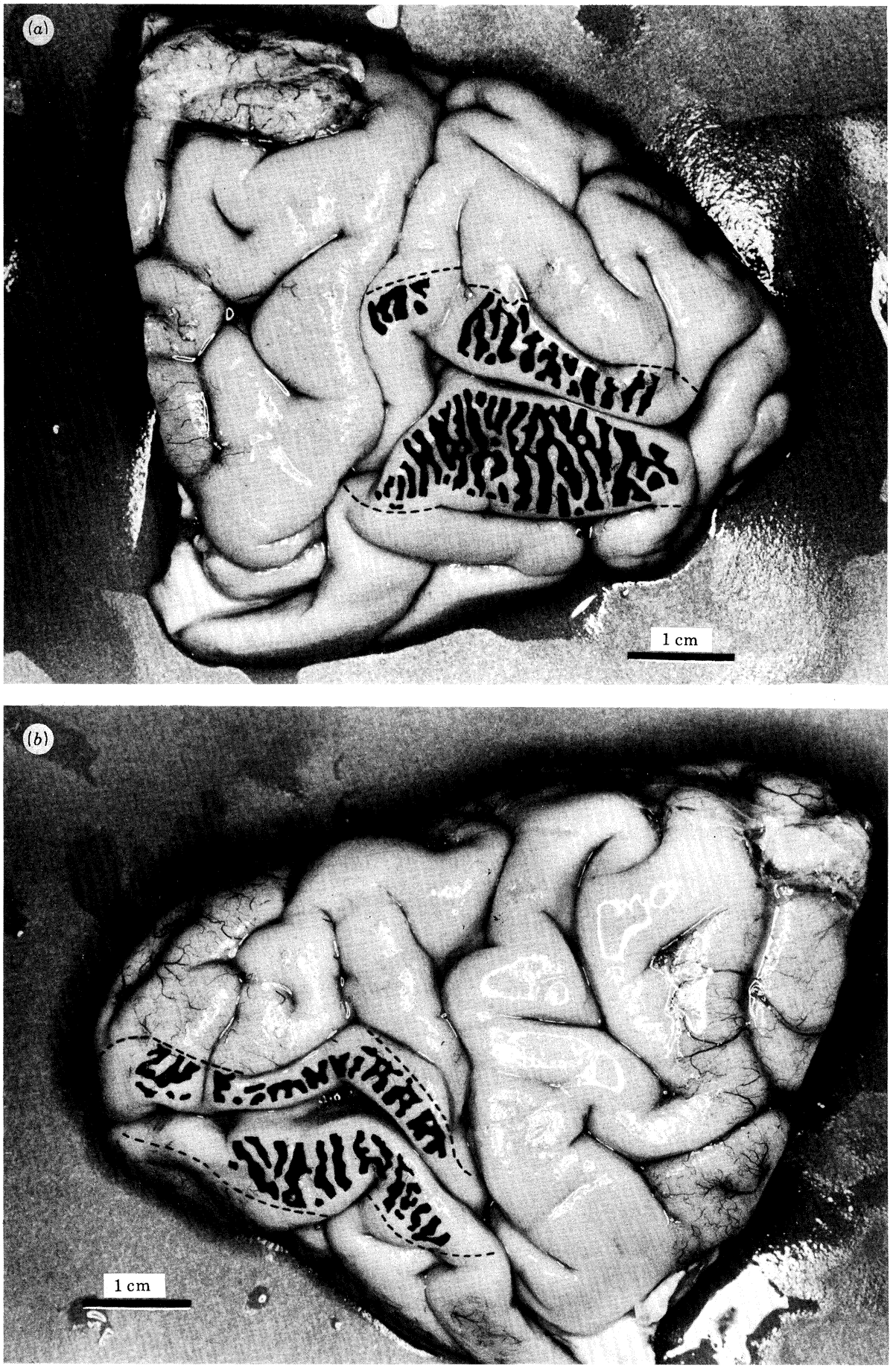

FIGURE 15. For description see p. 265.

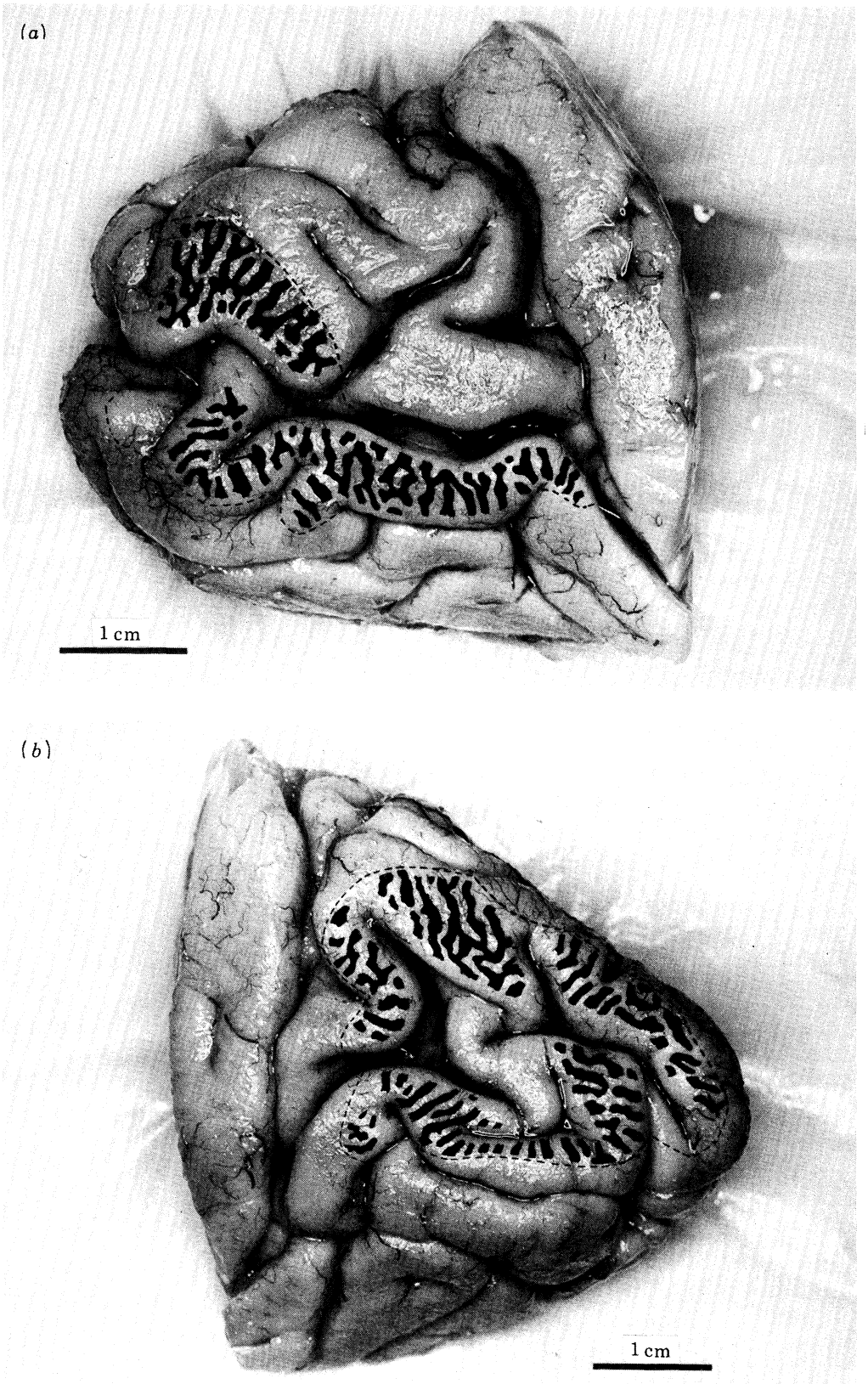

FIGURE 16. (*a*) Left and (*b*) right hemispheres from a 75 year old woman whose left eye was removed ten years before death showing superimposed pattern of ocular dominance columns in striate cortex. Again, columns are generally oriented perpendicular to the 17–18 boundary and appear as irregular slabs, averaging about 1 mm wide. Note how variable the pattern of sulci and gyri is from specimen to specimen: in (*b*) the calcarine sulcus is actually broken into two separate portions by a bridge of tissue.

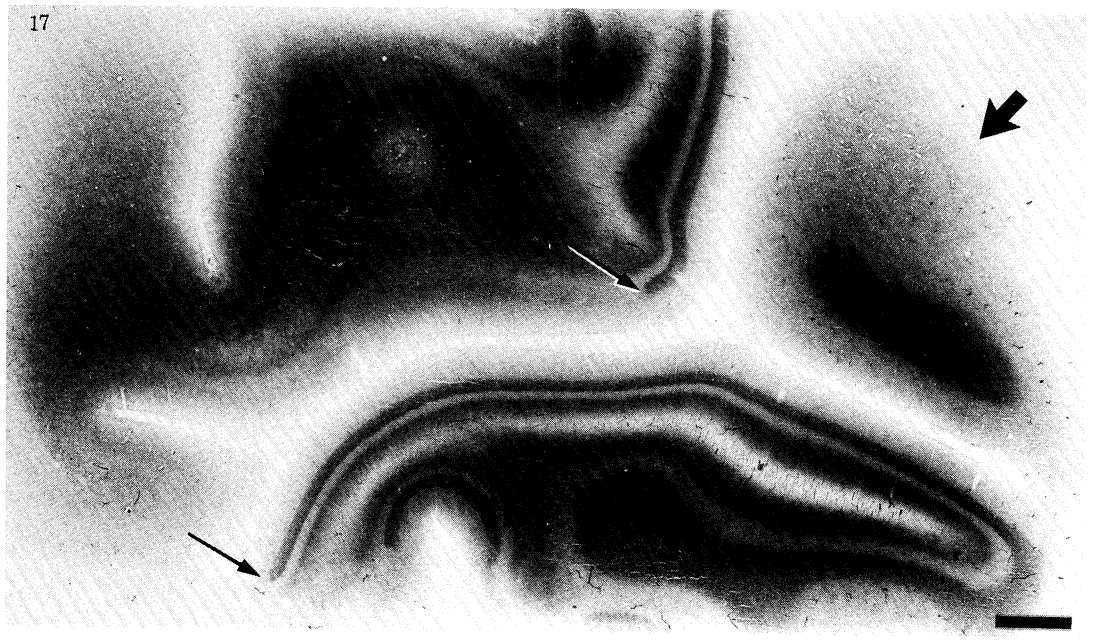

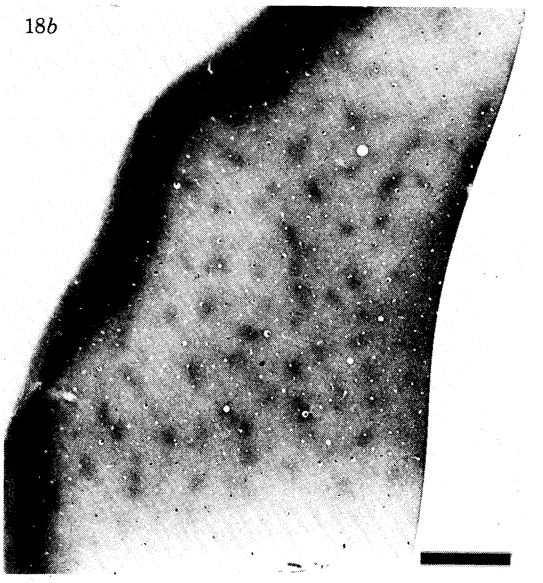

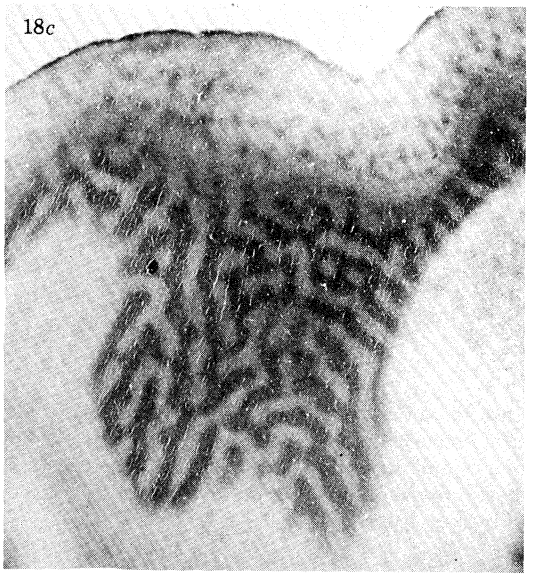

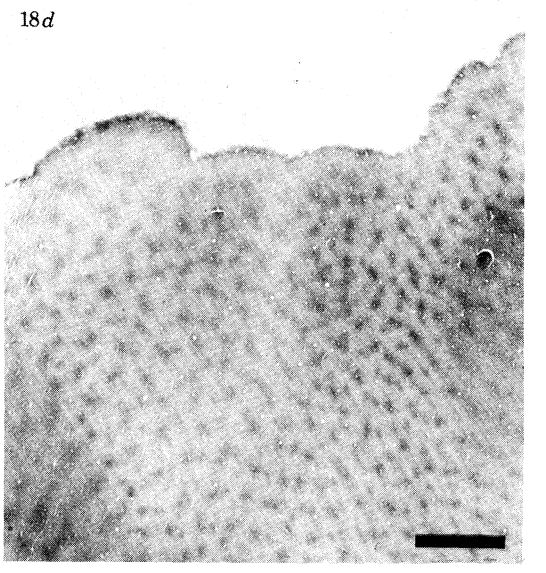

FIGURES 17 AND 18. For description see opposite.

FIGURE 14. Reconstruction of the pattern of ocular dominance columns over the medial face of the right hemisphere from the case illustrated in figure 10*b*; the region of the photomontage is to the lower right. Dotted lines indicate the 17–18 border; black columns correspond to the intact eye. Reconstruction was prepared by sketching pattern of columns in 62 serial sections viewed at low power in a Bausch & Lomb microscope projector.

islands. Nevertheless, there is an overall tendency for the columns to form roughly parallel slabs, about 1 mm wide, oriented perpendicular to the 17–18 border.

The patterns reconstructed in figures 15 and 16 may not be representative of the appearance of ocular dominance columns in normal human striate cortex. After enucleation the normal pattern might be distorted by expansion of ocular dominance columns belonging to the remaining eye. Therefore we made measurements of the areas of normal and enucleate eye dominance columns in both cases (Table 2). The measurements indicate that the columns

DESCRIPTION OF PLATES 12 AND 14

FIGURE 15 (*a*) Reconstruction in figure 14 superimposed photographically on a picture taken at autopsy of the right hemisphere before processing. Correct alignment was accomplished by referring to needle holes drilled before processing through embedded block of tissue. The dotted lines mark the 17–18 border, that is visible on the surface in some areas, and hidden in accessory sulci elsewhere. The calcarine fissure separates the upper and lower portions of the reconstruction; anteriorly it meets the parietooccipital sulcus. In blank areas within the confines of the dotted lines the pattern of columns could not be determined because the plane of section was too oblique; in other regions the columns disappear into the depths of various sulci. Columns appear quite irregular, but tend to intersect the 17–18 border at right angles.

(*b*) Left hemisphere, ipsilateral to the enucleated eye. Histological sections through this block were illustrated in figure 8; less of the column pattern could be reconstructed on this side.

FIGURE 17. Parasagittal section cut parallel to the medial face of the right occipital lobe in a six month old baby; posterior pole is to the far right. Layer IV appears as a prominent dark band of cytochrome oxidase activity; 17–18 border is marked at two points by thin arrows. Where section passes through layers II and III faint patches are visible (fat arrow) surrounding a region of intense homogeneous staining in layer IV. In the infant brain the patches are smaller and more closely spaced; total surface area of striate cortex is also much less compared with the adult. Scale = 2 mm.

FIGURE 18. Comparison of ocular dominance columns and patches in human and macaque striate cortex.

(*a*) Cytochrome oxidase stained section showing ocular dominance columns in layer IVc from the case illustrated in figure 16.

(*b*) Section cut 450 μm more superficially from the same block showing patches in layer III. As in figure 11, the patches in register with dark ocular dominance columns in IVc stain more darkly in layer III.

(*c*) Cytochrome oxidase stained section from a macaque monkey monocularly enucleated two weeks before death showing ocular dominance columns in layer IVc.

(*d*) Patches from same block in a section cut through layer III 375 μm more superficially. As in the human, patches located over darker columns in IVc stain more intensely for cytochrome oxidase. All four panels are reproduced at exactly the same magnification. Compared with the macaque, the ocular dominance columns in the human are about three times as wide, about 1 mm across as opposed to about 350 μm; otherwise they are strikingly similar in appearance. Likewise, the patches in the human are several times larger and more widely spaced than in the macaque. Scale = 2 mm.

corresponding to the remaining eye are very slightly greater in area. If the degenerative changes seen in enucleate-eye columns in the Nissl stain are considered, some mild contraction of these columns would not be surprising. However, the effects we see are so small that it seems that even 20 or more years after loss of one eye the ocular dominance columns respect their original boundaries in IV c_β.

TABLE 2. AREAS OF NORMAL AND ENUCLEATE EYE DOMINANCE COLUMNS

figure 15	(*a*) right cortex	%	(*b*) left cortex	%
enucleate eye columns	168 mm²	46	103 mm²	47
normal eye columns	200 mm²	54	117 mm²	53
total area:	368 mm²		220 mm²	
figure 16	(*a*) left cortex	%	(*b*) right cortex	%
enucleate eye columns	106 mm²	48	132 mm²	50
normal eye columns	114 mm²	52	132 mm²	50
total area:	220 mm²		264 mm²	

We were able to reconstruct only about 200–400 mm² of striate cortex in each case (table 2), mostly along the medial face of the occipital lobe where the columns are cut tangentially in layer IV in parasagittal section, providing an *en face* view of their pattern. The total area of human striate cortex is estimated to be about 3450 mm² (Brodmann 1911); thus we have reconstructed only a disappointing 10% or so of the column pattern in each hemisphere. We did cut serial sections completely through each lobe, about 300 are required to reach the bottom of the calcarine sulcus, and have verified that ocular dominance columns are visible throughout striate cortex except in a narrow region anteriorly that, it is presumed, corresponds to the monocular crescent; we have not succeeded in locating the optic disc representation unambiguously. Where the sulcal pattern folds to create small ledges and shelves we see the pattern of the ocular dominance columns, but are not able to piece together these isolated fragments meaningfully. Recently Connolly *et al.* (1982) have managed to reconstruct the entire pattern of ocular dominance columns in the macaque from a complete set of serial sections by aid of a computer. Such an approach might be feasible in the human striate cortex.

(*d*) *Normal development of the patches in striate cortex*

We examined cytochrome oxidase staining in striate cortex from several perinatal cases to determine when the patches develop in human brain. In a six month old foetus the boundary between striate and extrastriate cortex could be recognized on the basis of the characteristic dark band of staining in layer IV, but the laminar pattern of cytochrome oxidase activity was still quite rudimentary and patches were definitely not present (not illustrated). Cytochrome oxidase staining was tested in two babies who died the day after birth. Although satisfactory histology and enzyme reactivity was obtained, in neither case were we able to detect patches (not illustrated).

The right occipital lobe from a six month old baby with Down's syndrome who died after surgery to repair a heart defect is shown in figure 17, plate 14. In this case the laminar pattern of cytochrome oxidase activity looks quite mature and the 17–18 border is obvious. In tangential sections passing through the upper layers a faint pattern of patches is visible. The

patches are smaller and more closely spaced than those in adults, indeed the entire surface area of striate cortex is less. It is presumed that, as the cortex grows and expands, the patches increase proportionately in size and become more widely separated.

4. Discussion

(*a*) *Comparison between macaque and human striate cortex*

Application of the cytochrome oxidase stain to the human brain has permitted us to verify that certain basic cytoarchitectonic features of macaque striate cortex are also present in human striate cortex. There is a similar network of patches, larger and more widely spaced, but still generally organized into parallel rows running perpendicular to the 17–18 border. In many specimens the patches seem to form a more irregular pattern than in the macaque. This impression may be because we have reconstructed only smaller fragments of their overall pattern.

The cytochrome oxidase stain reveals a few interesting discrepancies between human and macaque in laminar distribution of enzyme activity. An upper tier of geniculate afferents in layer IVa, ending in a honeycomb network stained by cytochrome oxidase in the macaque monkey, appears to be lacking in man. Furthermore, in man the patches are more distinctly labelled in IVb and are even visible in IVc_{α}, where they seem to be absent in the macaque. The pattern of cytochrome oxidase staining in the owl monkey also differs from the macaque in these respects (Horton 1984). Apparently the details of the laminar pattern of geniculate input and cytochrome oxidase activity may show minor variations in different primate species. The key point is that all primates, including man, appear to have patches in primary visual cortex. Since the patches in layers II and III of the monkey are directly innervated by the lateral geniculate nucleus (Horton 1984; Fitzpatrick *et al.* 1983), it is likely that the upper layer patches in man also receive a direct geniculate projection.

Examination of cytochrome oxidase activity in three patients who lost one eye many years before death has confirmed that ocular dominance columns are present in human striate cortex. They are about 1 mm wide on average, in good agreement with Schwartz's (1980) prediction based upon theoretical calculations, and with the spacing between silver bands found by Hitchcock & Hickey (1980). In man the ocular dominance columns are very similar in pattern to the macaque's, at least near the 17–18 border. Furthermore, each ocular dominance columns lies in register with a row of patches outside IVc_{β}; enucleation causes the patches in every other row to fade and shrink, matching a pale column in IVc belonging to the missing eye. Hendrickson *et al.* (1978) have proposed that ocular dominance columns are a special feature of old world monkeys, lacking in new world monkeys. While Hendrickson *et al.* noted exceptions to this rule (Florence & Casagrande 1978), it does appear that ocular dominance columns are better developed and more strictly segregated in old world monkeys. It is thus not surprising that ocular dominance columns in the human and the macaque appear so alike, since old world monkeys, apes, and man are thought to share common evolutionary origins in the late Eocene. Probably macaque visual cortex is more similar to human visual cortex than, for example, the visual cortex of the squirrel monkey which contains such poorly developed dominance columns they have defied clear anatomical demonstration.

The difference in scale between macaque and human striate cortex is impressive. Figure 18 shows the ocular dominance columns and patches in both human and macaque at precisely

the same magnification. The ocular dominance columns are about 1 mm wide in the human, compared with 0.35 mm in the macaque; the patches are also several times larger. Although measurements are difficult to make accurately because the patches often appear rather poorly separated, we find approximately one patch per 0.6–0.8 mm^2 in human visual cortex near the foveal representation, about one third of the density in the macaque (one patch per 0.2 mm^2). Figures for the total surface area of striate cortex in man and macaque range widely, reflecting variation in specimens and in techniques of histology and measurement. If various estimates are averaged, the total surface area of human striate cortex (3000–3600 mm^2) is about three times greater than the surface area of macaque striate cortex (1000–1400 mm^2). Therefore, the number of ocular dominance hypercolumns and patches is probably quite similar in man and macaque. If we allow for the higher density of patches in peripheral cortex (Horton 1983), there are probably 7000–9000 patches present in both species. It may be that the number of patches is conserved across primate species. In the baboon, with an area of striate cortex between that of man and macaque, the patches are also intermediate in size and spacing. However, in squirrel monkey there is about one patch per 0.22 mm^2: given a total of about 720 mm^2 of striate cortex (Cowey 1964) only about 3300 patches are present in this species, about half the number found in the macaque or human. This discrepancy might be because of the near absence of ocular dominance columns in the squirrel monkey, that makes having a patch for each eye dominance column unnecessary. Clearly though, despite the similar number of patches in some species, the number present may vary widely from species to species.

Hubel & Wiesel (1977) have postulated that the visual field is analysed in a piecemeal fashion in macaque striate cortex by blocks of tissue composed of multiple overlapping hypercolumns. The cytochrome oxidase patches may be the anatomical substrate for these proposed modules. Given that the surface area of striate cortex is about three times greater in man, we might have expected three times as many patches, each the same size as a patch in the macaque. Instead, we found that the number of patches is about the same but each patch is amplified in scale by three times. This means that a patch in human striate cortex is responsible for analysing a portion of visual field measuring about the same area in degrees as a patch in the macaque, if a corresponding retinotopic location is assumed. Thus in the human a much larger block of tissue is available to process information from an equivalent portion of visual field. This cortical block is not only three times greater in area, and 10–30% thicker, but contains cells that are larger. Layer IVc stellate cells in normal-eye columns in macaque measure $34.8 \pm 0.89\ \mu m^2$ (Haseltine *et al.* 1979), compared with $57.3 \pm 1.35\ \mu m^2$ in the human, a difference that is hard to ascribe entirely to tissue shrinkage or variation in histological methods. The larger module of the human receives a projection from roughly the same number of geniculate neurons as in the macaque. Le Gros Clark (1941) estimates that each mm^2 of macaque cortex receives 1350 optic radiation fibres (270 per 0.2 mm^2). Since the human lateral geniculate contains about the same number of cells, or less (Balado & Frauke 1937), only about 500 project to each mm^2 (300–400 per 0.6–0.8 mm^2) of cortex. The conclusion follows that the human and macaque module receive a similar thalamic input, but the human module has more cells and larger cells, probably making more extensive intracortical and intercortical connections. The significance of this extra cortical machinery for human vision is unknown. With behavioural testing it has been difficult to demonstrate a clear difference between man and macaque in contrast sensitivity, grating acuity, or hue discrimination. The

superior ability of man to interpret visual input is usually ascribed to a more highly developed association visual cortex; perhaps the increased area of striate cortex should also be considered in this regard.

(*b*) *Significance for neuropathology*

Neurons in the human lateral geniculate nucleus stain intensely for cytochrome oxidase activity. These cells project primarily to layer IV c of striate cortex, which explains in part why this layer appears so darkly stained in normal specimens. After eye removal anterograde degeneration occurs in the human lateral geniculate (Le Gros Clark 1932). Measurements by Goldby (1957) have indicated a 35–45% decrease in mean cell area and a 50% drop in cell population in denervated laminae. We have observed a sharp decrease in cytochrome oxidase activity in cell bodies and neuropil of atrophic laminae. It is presumed that there is a corresponding loss of geniculate terminals in cortex and weaker cytochrome oxidase activity in surviving terminals. As a result, ocular dominance columns corresponding to the missing eye appear visible as lighter staining slabs of cortex in layer IV c. However, geniculate terminals make up only a small fraction of the axon terminals in any cortical layer, even in IV c (Garey & Powell 1971), so this probably does not account entirely for the contrast in cytochrome oxidase staining between normal and enucleate-eye columns. Changes probably also occur in levels of cytochrome oxidase within cortical cells, particularly in post-synaptic dendrites receiving geniculate afferents.

Our measurements showed significant atrophy of layer IV c stellate cell bodies. Probably this is accompanied by contraction of their dendritic and axonal processes with a drop in their cytochrome oxidase content. This atrophy of cortical cells, combined with loss of geniculate terminals, causes the neuropil to shrink, thereby increasing the density of cell bodies in enucleate-eye columns. This explains why ocular dominance columns that stain more darkly with cresyl violet match columns exhibiting weaker cytochrome oxidase activity. We also noticed cortical degeneration in the upper layers, strengthening our suspicion that the patches in the human are directly innervated by the lateral geniculate. We presume that degenerative processes similar to those at work in layer IV c also play a role in the loss of cytochrome oxidase activity in patches belonging to the missing eye. Finally, it should be noted that merely closing an eye in the macaque will cause cytochrome oxidase levels in the cortex to fall, without development of degenerative changes in the geniculate or cortex (Horton 1984). Therefore, the appearance of the cortex after eye removal reflects changes in cytochrome oxidase activity caused by neuronal degeneration combined with effects caused by functional neuronal inactivity.

Transneuronal degeneration in the lateral geniculate nucleus after eye removal is obvious in either the Nissl stain or the cytochrome oxidase stain. On the other hand, secondary transneuronal degeneration in the cortex appears quite subtle in the Nissl stain. Although neuropathologists have examined Nissl stained specimens of calcarine cortex from cases involving monocular enucleation for many years it was not until Haseltine *et al.* (1979) reported dark and light Nissl bands in striate cortex of an enucleated macaque that secondary anterograde transneuronal atrophy was clearly demonstrated in the visual cortex. It must be a commonly occurring process in many regions of cerebral cortex after stroke, degenerative diseases, and other lesions of the nervous system. Probably it has been reported so infrequently

because one is usually unsure what sort of changes to search for, and because these changes are so difficult to detect in the Nissl stain. In this latter respect, cytochrome oxidase histochemistry may prove valuable as a routine technique for evaluating central nervous system pathology. The ocular dominance columns appear faint in the Nissl stain after eye removal, but can hardly be missed in cytochrome oxidase stained material. Changes in cytochrome oxidase levels often develop more rapidly after a lesion – in just a matter of days – than changes in the Nissl stain. Furthermore, cytochrome oxidase levels are altered merely by sensory deprivation (Horton 1983), even in the absence of any change detectable in the Nissl. The cytochrome oxidase technique is easy to use, reliable, inexpensive, and can be applied to tissue up to 24 h *post mortem*. It has been used recently in a rare case of congenital anophthalmia to demonstrate abnormalities in striate cortex not apparent by any other technique (Brunquell *et al.* 1983).

Progress has been made developing *in vivo* techniques like positron emission tomography for mapping metabolic activity in the human brain. However, theoretical limitations make it seem doubtful the resolution will become detailed enough to allow cytoarchitectonic structures as small as the ocular dominance columns in striate cortex to become visible. Most elements of the functional architecture in any cortical area, such as the patches in striate cortex, are of the order of 100–1000 μm in size, beyond the range promised by these techniques. However, it will soon be possible to begin mapping the boundaries of various cortical regions using positron emission tomography. This task will be complicated by the fact that many more regions exist than the 47 originally distinguished by Brodmann on the basis of Nissl cytoarchitectonics. Studies in the cat and monkey, recently reviewed by Van Essen (1979), suggest there may turn out to be more than a dozen areas in visual cortex alone, each containing a separate map of the visual field. It may be possible to delineate these regions in the human brain if they can be associated with characteristic patterns of cytochrome oxidase staining in normal specimens. V2 in the macaque is distinguished by a regular pattern of parallel stripes, quite distinct from the system of patches seen in V1 (striate cortex). In the human we have also noticed this pattern in V2; it may help to locate the border between V2 and association visual cortex lying beyond. We can expect many of our findings in the macaque to extend to man in areas like visual cortex or somatosensory cortex. It will be interesting to examine cytochrome oxidase patterns in Wernicke's area, or Broca's area, regions lacking a well developed counterpart in lesser primates.

(*c*) *Development of patches in human striate cortex*

In the macaque monkey, patches are present several weeks before birth, although they appear much fainter than in adults (Horton 1984). The patches undoubtedly develop over a period of weeks, gradually appearing more and more distinct in the cytochrome oxidase stain. We suspect that if more human cases are examined the patches will be detected before the age of six months.

So far we have examined the pattern of ocular dominance columns only in adults who lost one eye as adults. Hubel *et al.* (1977) have demonstrated in the macaque that if one eye is lost early in life, geniculate terminals driven by the remaining eye in layer IVc of the cortex sprout to enlarge the width of normal eye columns at the expense of those corresponding to the missing eye. Enucleation performed after the 'critical period', when this capacity for compensatory change by geniculate terminals is lost, results in a normal pattern of ocular dominance columns

in the cortex. LeVay *et al.* (1980) have determined that in macaque striate cortex plasticity for sprouting of geniculate terminals is preserved up to four months after birth. By examining a series of cases from adults who lost one eye at different childhood ages it should be possible to pinpoint the timing of this period of anatomical plasticity in man. Because of the relative immaturity of visually guided behaviour at birth in the human compared with the macaque, and the surprisingly late age at which some benefit is obtained by eye patching in treatment of amblyopia, the development of patches and ocular dominance columns may occur in man at a slightly later time.

We thank Dr Torsten N. Wiesel and Dr Simon LeVay for their helpful comments on the manuscript. Assistance with photography was provided by Marc Peloquin. The Departments of Pathology at New England Deaconess Hospital, Children's Hospital, and Mass General Hospital and U.S.P.H.S. Medical Scientist Training Grant GM07753 (J.C.H.) are gratefully acknowledged.

References

Balado, M. & Franke, E. 1937 *Das Corpus Geniculatum Externum.* Berlin: Julius Springer.

Brodmann, K. 1911 Neue Probleme der Rindenloth. *Neurol. Centrabl.* **30**, 696.

Brunquell, P. J., Papale, J. J., Horton, J. C., Williams, R. S., Zgrabik, M. J., Albert, D. M. & Hedley-Whyte, E. T. 1983 Sex-linked hereditary bilateral anophthalmos: pathologic and radiologic correlation. *Arch Ophthal.* (In the press.)

Clark, W. E. L. G. 1932 A morphological study of the lateral geniculate body. *Br. J. Ophthal.* **16**, 264–284.

Clark, W. E. L. G. 1941 The laminar organization and cell content of the lateral geniculate body in the monkey. *J. Anat.* **75**, 419–434.

Connolly, M., LeVay, S. & Van Essen, D. C. 1982 The complete pattern of ocular dominance stripes in macaque striate cortex. *Soc. Neurosci.* **8**, 192.4.

Cotlier, E., Lieberman, T. W. & Gay, A. J. 1965 Dehydrogenases and diaphorases in monkey lateral geniculate body. *Arch. Neurol.* **12**, 295–299.

Cowey, A. 1964 Projection of the retina on to striate and prestriate cortex in the squirrel monkey, *Saimira sciureus. J. Neurophysiol.* **27**, 366–393.

Fitzpatrick, D., Itoh, K. & Diamond, I. T. 1983 The laminar organization of the lateral geniculate body and the striate cortex in the squirrel monkey (*Saimiri sciureus*). *J. Neurosci.* **3**, 673–702.

Florence, S. L. & Casagrande, V. A. 1978 A note on the evolution of ocular dominance columns in primates. *Invest. Ophthal.* Suppl. 291.

Frank, E., Harris, W. A. & Kennedy, M. B. 1980 Lysophosphatidyl choline facilitates labeling of CNS projections with horseradish peroxidase. *J. Neurol. Methods* **2**, 183–189.

Garey, L. J. & Powell, T. P. S. 1971 An experimental study of the termination of the lateral geniculo-cortical pathway in the cat and monkey. *Proc. R. Soc. Lond.* B **179**, 1–63.

Gay, A. L. & Silberberg, D. H. 1964 Histochemical correlates of transynaptic degeneration. *Arch. Neurol.* **10**, 85–90.

Goldby, F. 1957 A note on transneuronal atrophy in the human lateral geniculate body. *J. Neurol. Neurosurg. Psychiat.* **20**, 202–207.

Haseltine, E. C., DeBruyn, E. J. & Casagrande, V. A. 1979 Demonstration of ocular dominance columns in Nissl-stained sections of monkey visual cortex following enucleation. *Brain Res.* **176**, 153–158.

Hendrickson, A. E., Hunt, S. P. & Wu, J. Y. 1981 Immunocytochemical localization of glutamic acid decarboxylase in monkey striate cortex. *Nature, Lond.* **292**, 605–607.

Hendrickson, A. E., Wilson, J. R. & Ogren, M. P. 1978 The neuroanatomical organization of pathways between the dorsal lateral geniculate nucleus and visual cortex in Old World and New World primates. *J. comp. Neurol.* **182**, 123–136.

Hitchcock, P. F. & Hickey. T. L. 1980 Ocular dominance columns: evidence for their presence in humans. *Brain Res.* **182**, 176–179.

Horton, J. C. 1984 Cytochrome oxidase patches: a new cytoarchitectonic feature of monkey visual cortex. *Phil. Trans. R. Soc. Lond.* B **304**, 199–253.

Horton, J. C. & Hubel, D. H. 1980*a* Correlation of cytochrome oxidase staining with 2-deoxyglucose uptake in monkey visual cortex. *Arch. Biol. Med. Exp.* **13**, 12.

Horton, J. C. & Hubel, D. H. 1980*b* Cytochrome oxidase stain preferentially labels intersection of ocular dominance and vertical orientation columns in macaque striate cortex. *Soc. Neurosci.* **6**, 113.5.

Horton, J. C. & Hubel, D. H. 1981 Regular patchy distribution of cytochrome oxidase staining in primary visual cortex of macaque monkey. *Nature, Lond.* **292**, 762–764.

Hubel, D. H. & Wiesel, T. N. 1972 Laminar and columnar distribution of geniculo-cortical fibers in the macaque monkey. *J. comp. Neurol.* **146**, 421–450.

Hubel, D. H. & Wiesel, T. N. 1977 Functional architecture of macaque monkey visual cortex. *Proc. R. Soc. Lond.* B **198**, 1–59.

Hubel, D. H., Wiesel, T. N. & LeVay, S. 1977 Plasticity of ocular dominance columns in monkey striate cortex. *Phil. Trans. R. Soc. Lond.* B **278**, 377–409.

Humphrey, A. L. & Hendrickson, A. E. 1980 Radial zones of high metabolic activity in squirrel monkey striate cortex. *Soc. Neurosci.* **6**, 113.6.

Kennedy, C., Des Rosiers, M. H., Sakurada, O., Shinohara, O., Reivich, M., Jehle, J. W. & Sokoloff, L. 1976 Metabolic mapping of the primary visual system of the monkey by means of the autoradiographic [^{14}C]deoxyglucose technique. *Proc. natn. Acad. Sci. U.S.A.* **73**, 4230–4234.

LeVay, S., Hubel, D. H. & Wiesel, T. N. 1975 The pattern of ocular dominance columns in macaque visual cortex revealed by a reduced silver stain. *J. comp. Neurol.* **159**, 559–576.

LeVay, S., Wiesel, T. N. & Hubel, D. H. 1980 The development of ocular dominance columns in normal and visually deprived monkeys. *J. comp. Neurol.* **191**, 1–51.

Minkowski, M. 1920 Uber den Verlauf, die Endigung und die zentrale Reprasentation von gekreuzten und ungekreuzten Sehnervenfasern bei einigen Saugetieren und beim Menschen. *Schweiz. Arch. Neur. Psychiat.* **6**, 201–252.

Schwartz, E. L. 1980 Computational anatomy and functional architecture of striate cortex: a spatial mapping approach to perceptual coding. *Vision Res.* **20**, 645–669.

Seligman, A. M., Karnovsky, M. J., Wasserkrug, H. L. & Hanker, J. S. 1968 Nondroplet ultrastructural demonstration of cytochrome oxidase activity with a polymerizing osmiophilic reagent, diaminobenzidine (DAB). *J. Cell Biol.* **38**, 1–14.

Tootell, R. B. H., Silverman, M. S., De Valois, R. L. & Jacobs, G. H. 1983 Functional organization of the second cortical visual area in primates. *Science, N.Y.* **220**, 737–739.

Van Essen, D. C. 1979 Visual areas of the mammalian cerebral cortex. *A. Rev. Neurosci.* **2**, 227–263.

Weber, J. T., Kaas, J. H., Huerta, M. F. & Harting, J. K. 1977 Connections of the lateral geniculate nucleus (LGN) of the squirrel monkey. *Soc. Neurosci.* **3**, 1860.

Wiesel, T. N., Hubel, D. H. & Lam, D. M. K. 1974 Autoradiographic demonstration of ocular dominance columns in the monkey striate cortex by means of transneuronal transport. *Brain Res.* **79**, 273–279.

Wong-Riley, M. 1979 Changes in the visual system of monocularly sutured or enucleated kittens demonstrable with cytochrome oxidase histochemistry. *Brain Res.* **171**, 11–28.

Wong-Riley, M. T. T., Merzenich, M. M. & Leake, P. A. 1978 Changes in endogenous enzymatic reactivity to DAB induced by neuronal inactivity. *Brain Res.* **141**, 185–192.

Wong-Riley, M. T. T. & Welt, C. 1980 Histochemical changes in cytochrome oxidase of cortical barrels after vibrissal removal in neonatal and adult mice. *Proc. natn. Acad. Sci. U.S.A.* **77**, 2333–2337.

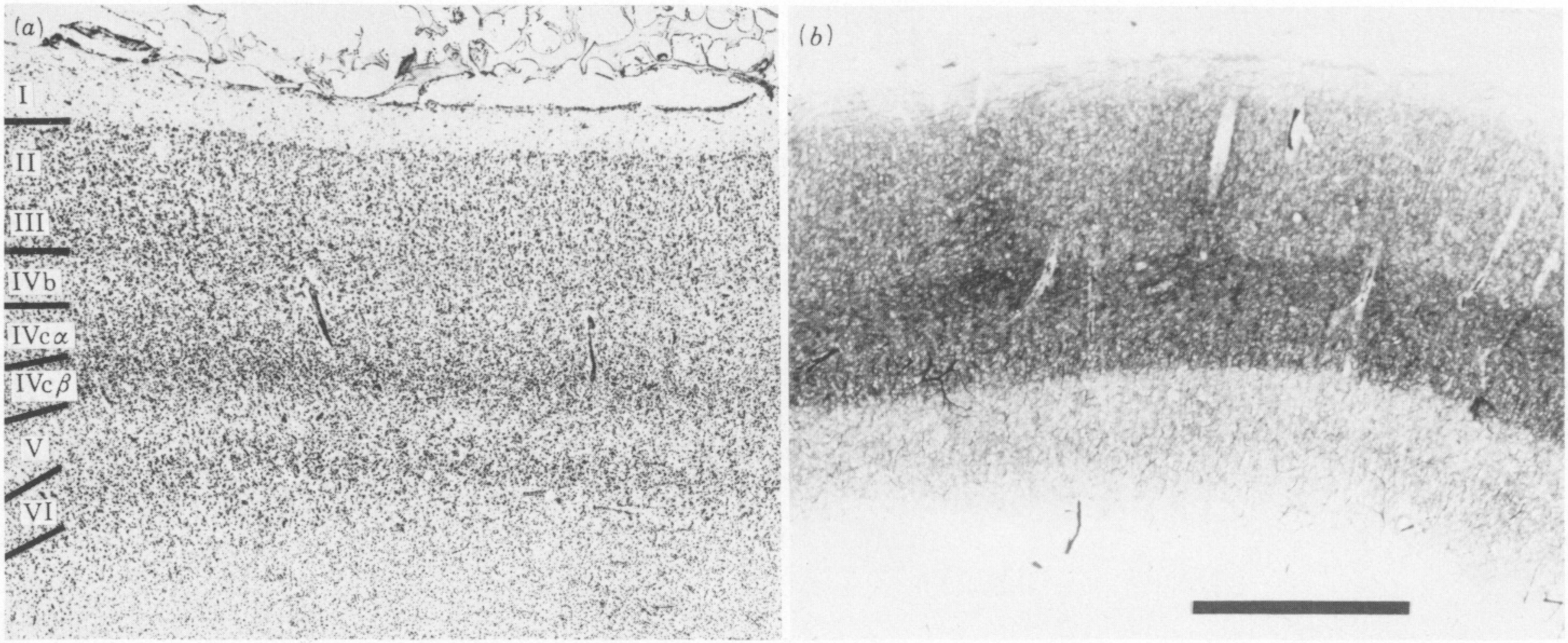

FIGURE 1. Coronal sections through normal human striate cortex (primary visual cortex, area 17) obtained *post mortem*.

(*a*) Cresyl violet stain shows classical appearance of the layers, with a densely cellular layer IVc and a relatively cell-sparse layer IVb above containing the stria of Gennari.

(*b*) An adjacent section stained for cytochrome oxidase shows a dense band in layer IVc, sharing a sharp lower border with layer V that stains more weakly. Note the absence of an 'upper tier' of intense cytochrome oxidase activity characteristic of layer IVa in a macaque. Staining is also surprisingly rich in layer IVb.

(*c*) In the cytochrome oxidase stain periodic vertical columns of enhanced enzyme activity are visible in the upper layers, spaced about 1 mm apart (arrows). Scale = 1 mm.

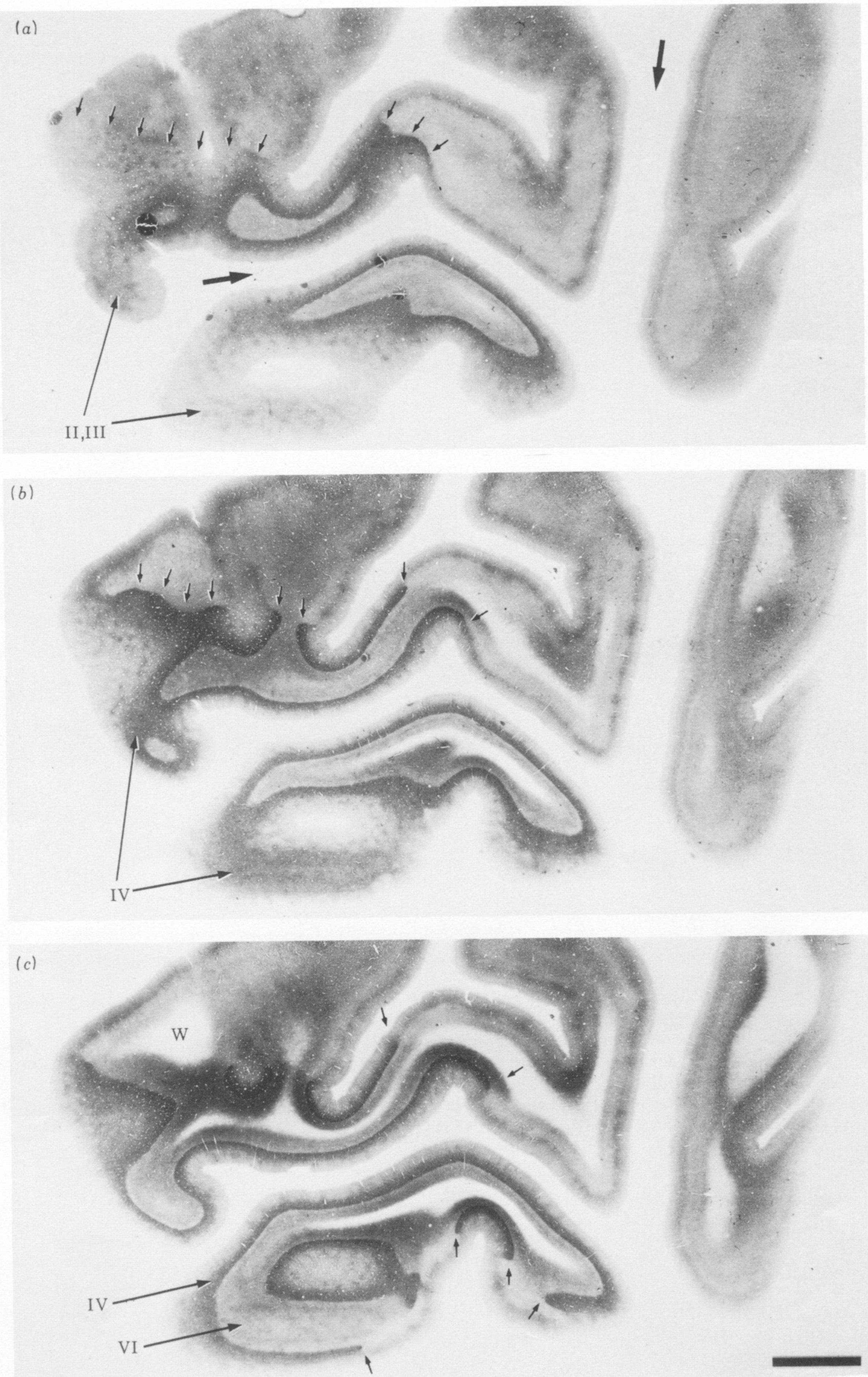

FIGURE 2. For description see p. 260.

3

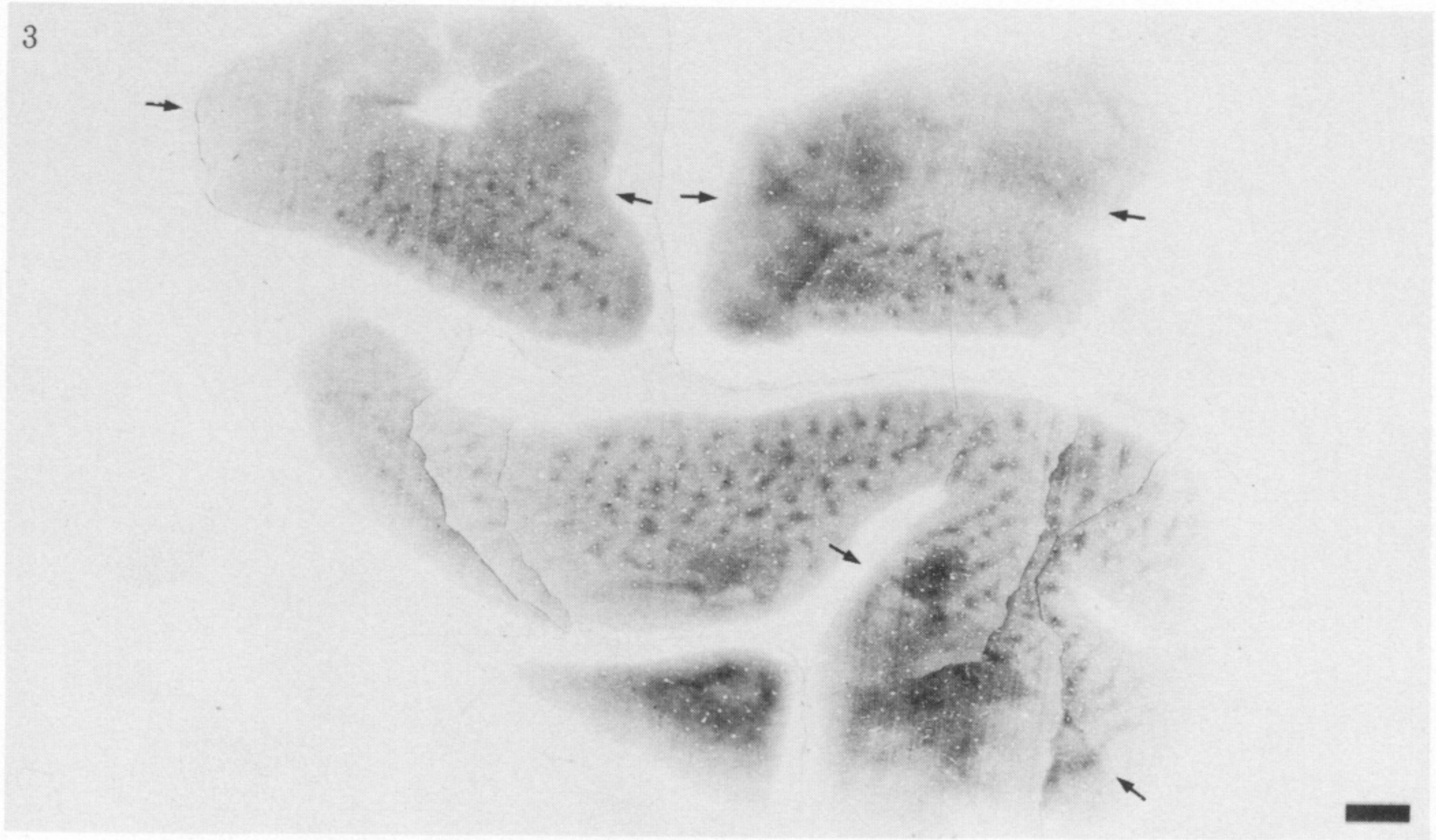

4

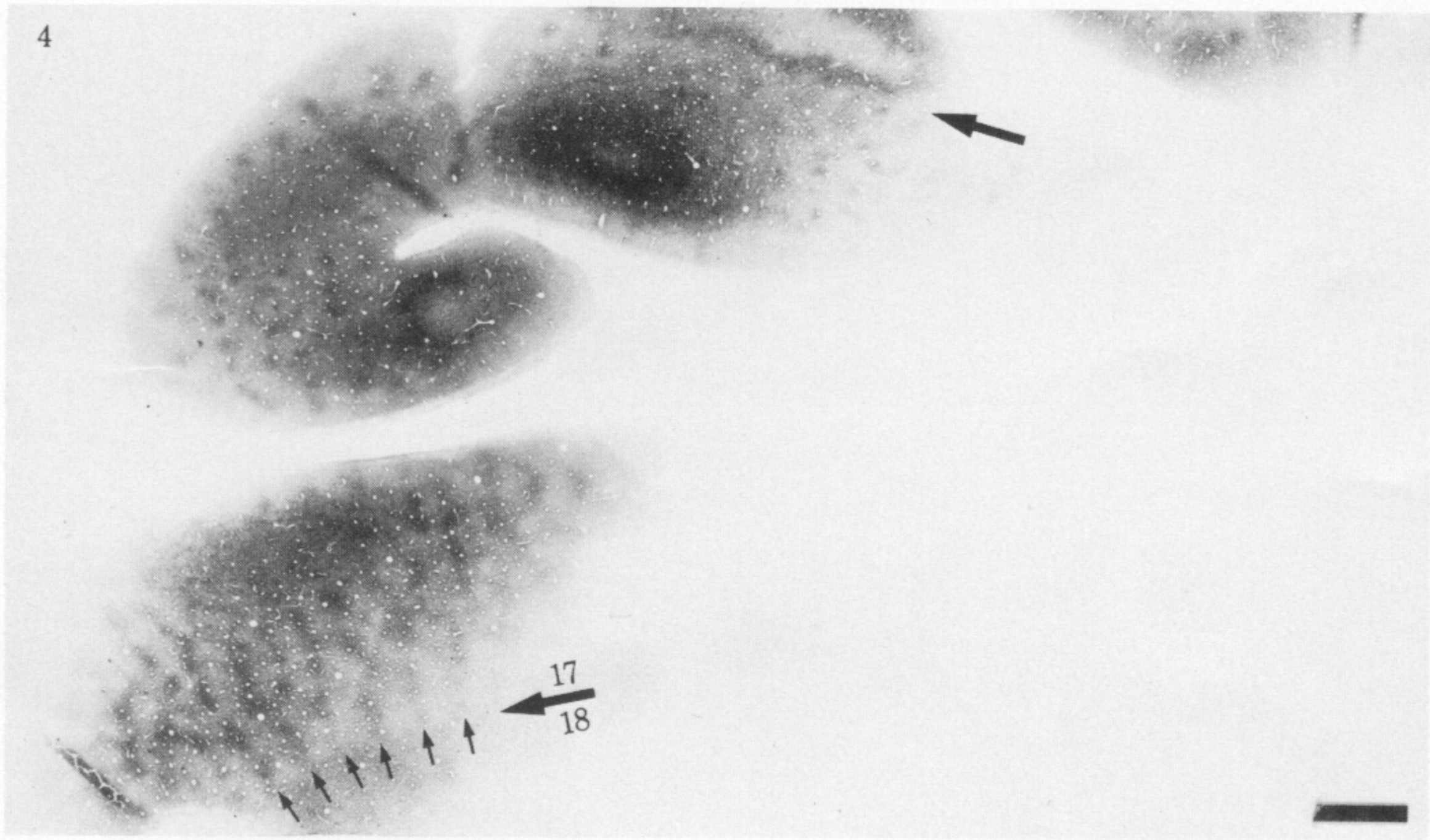

5*a*

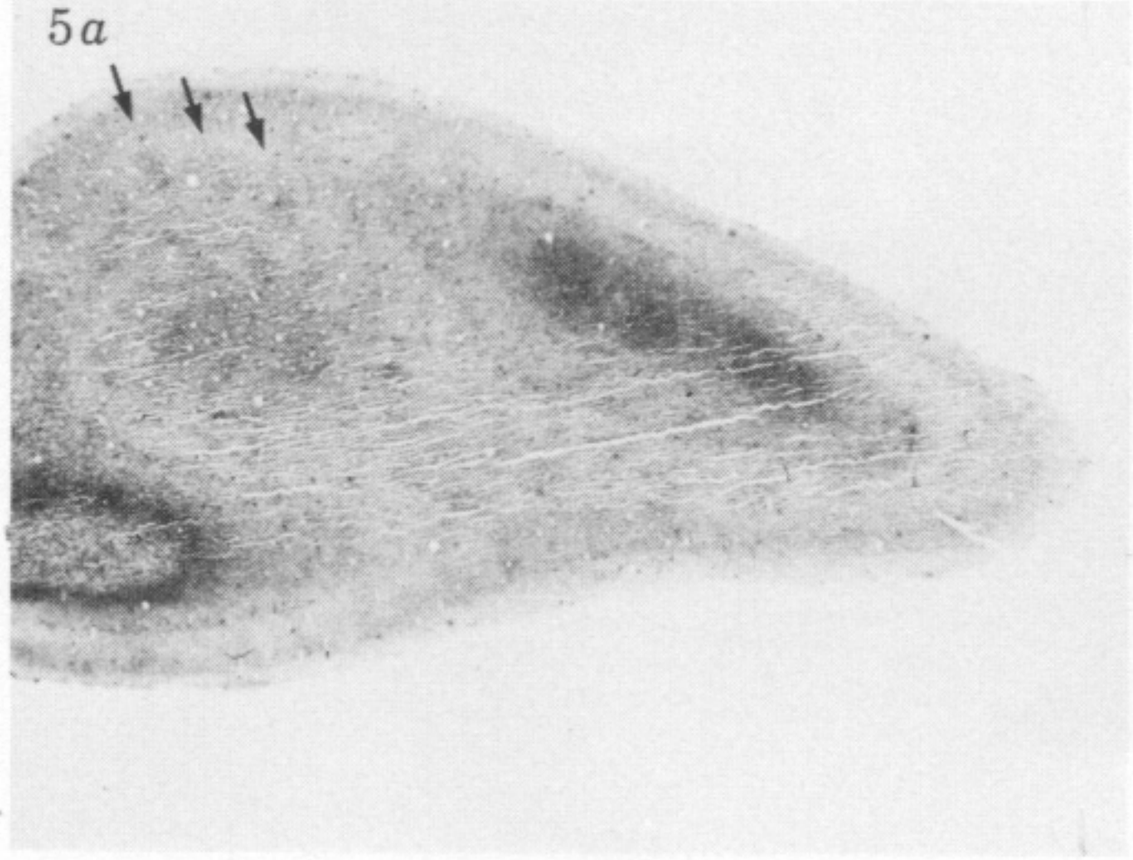

5*b*

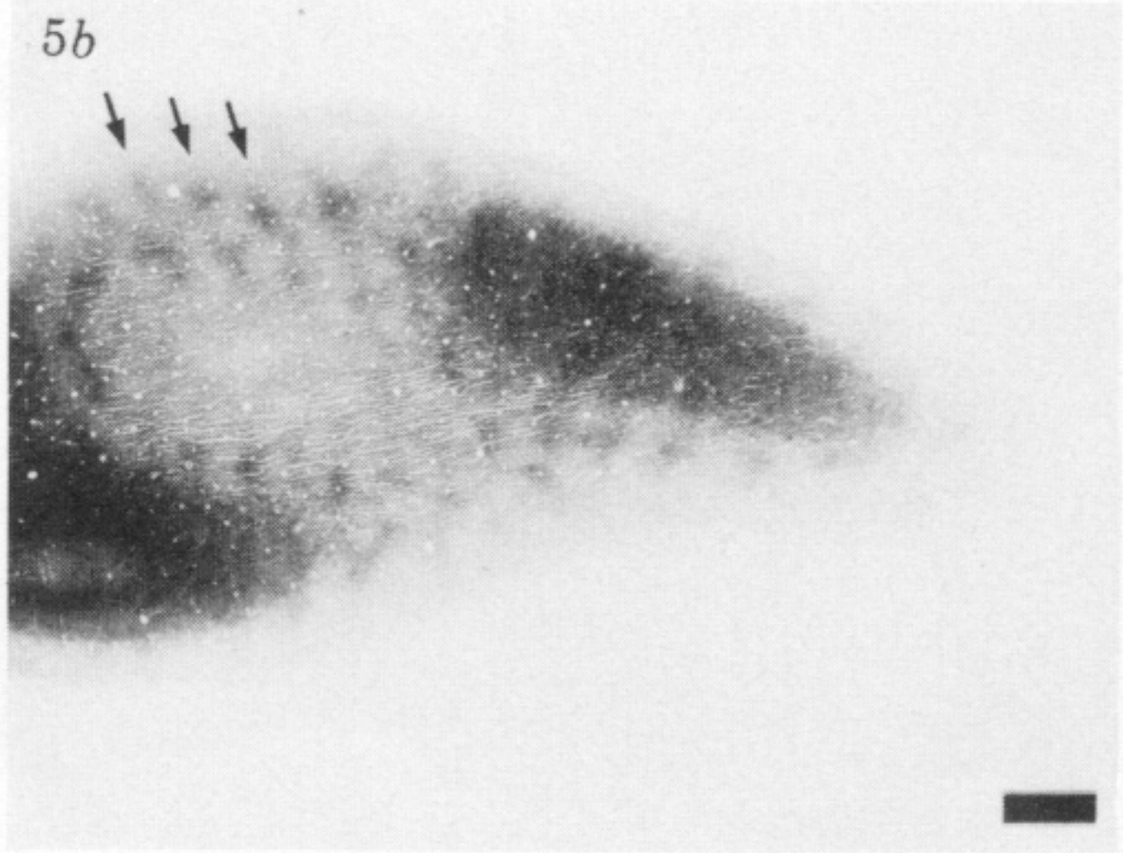

FIGURES 3–5. For description see p. 260.

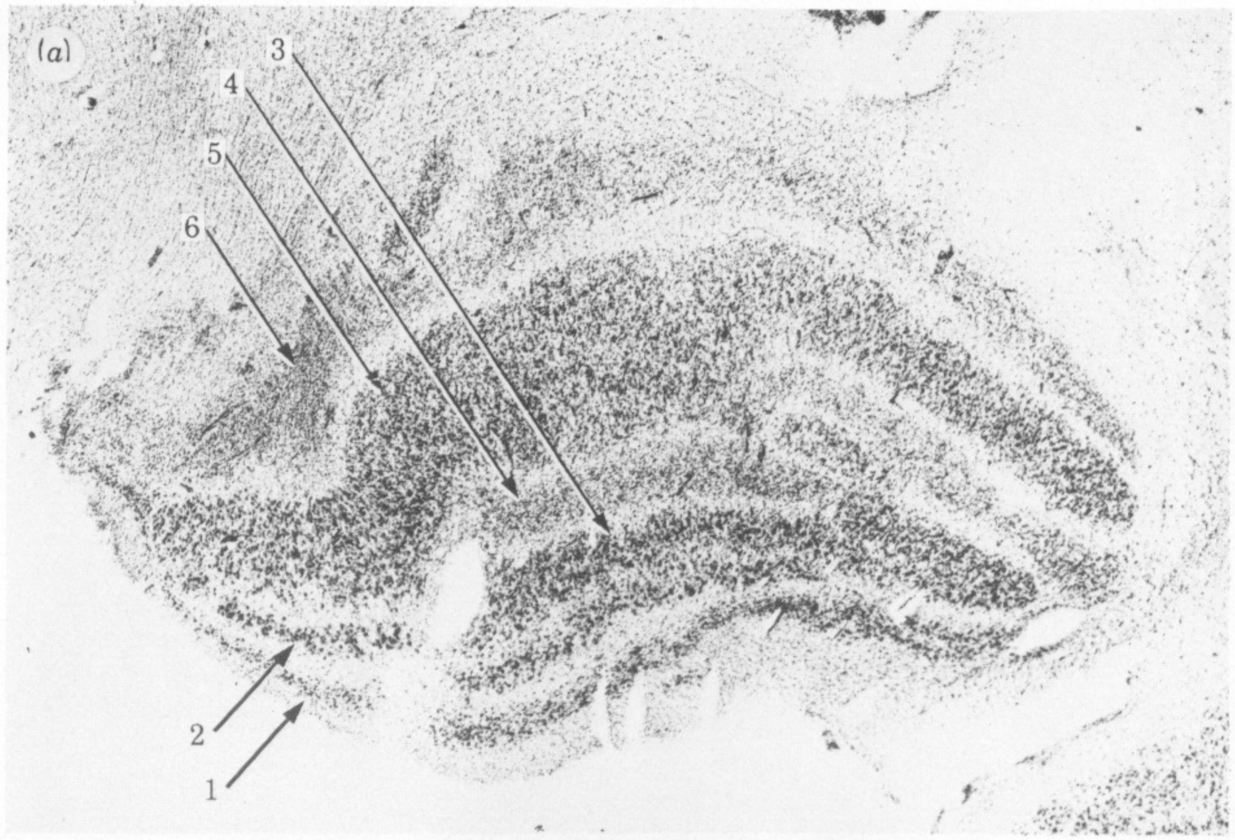

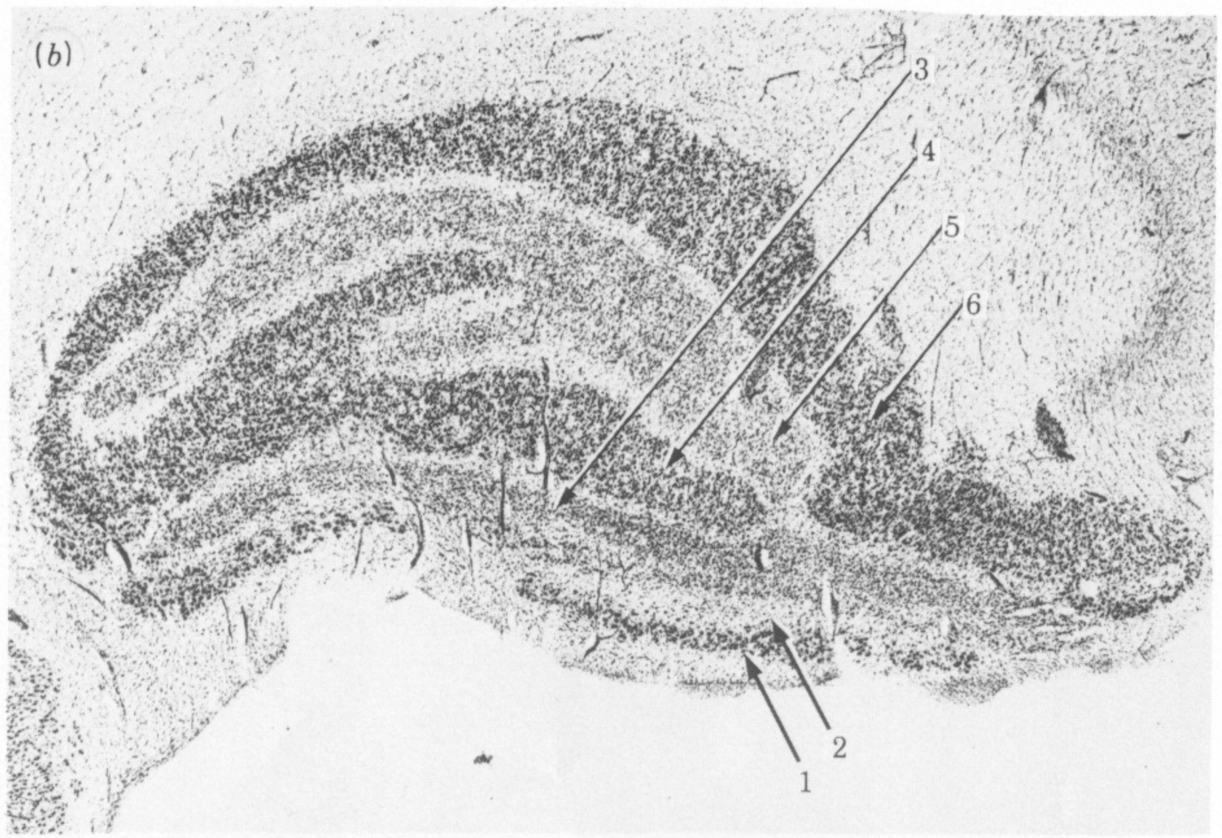

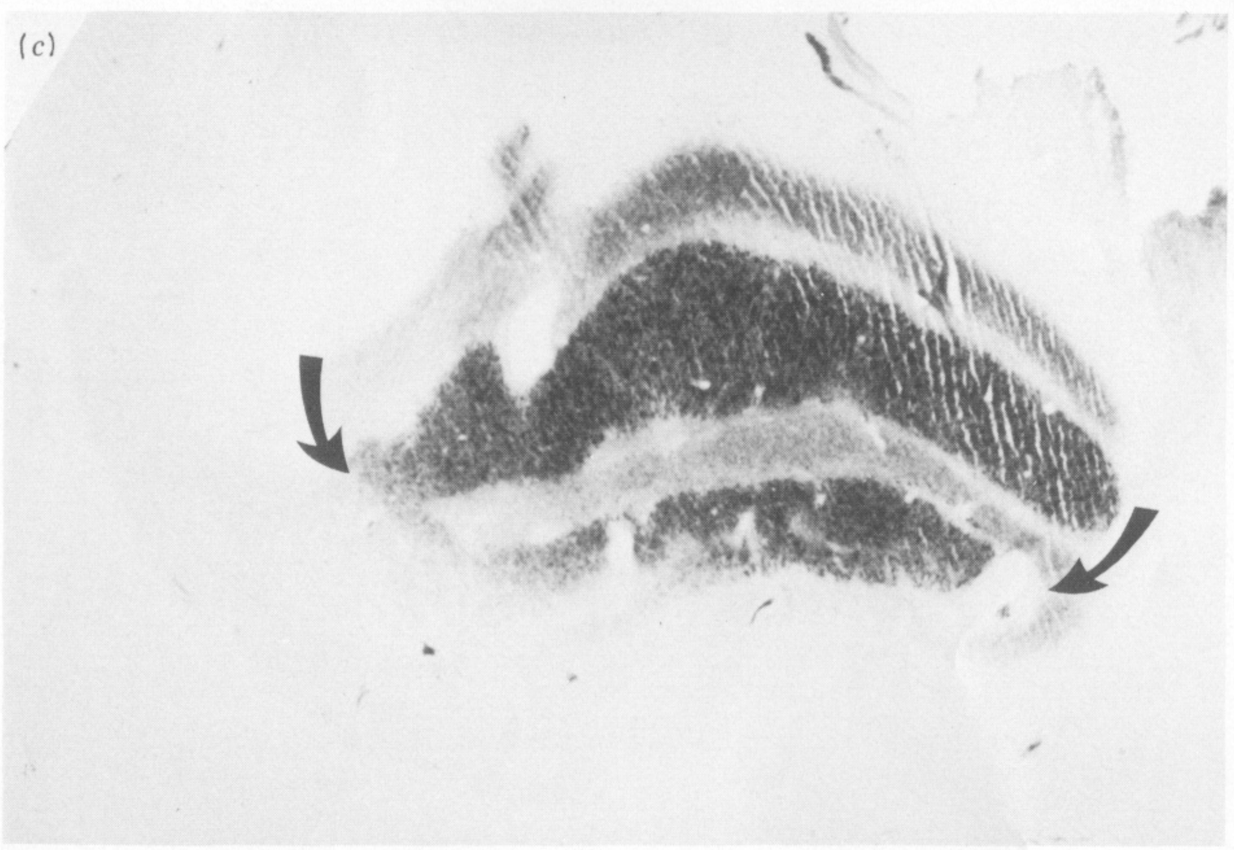

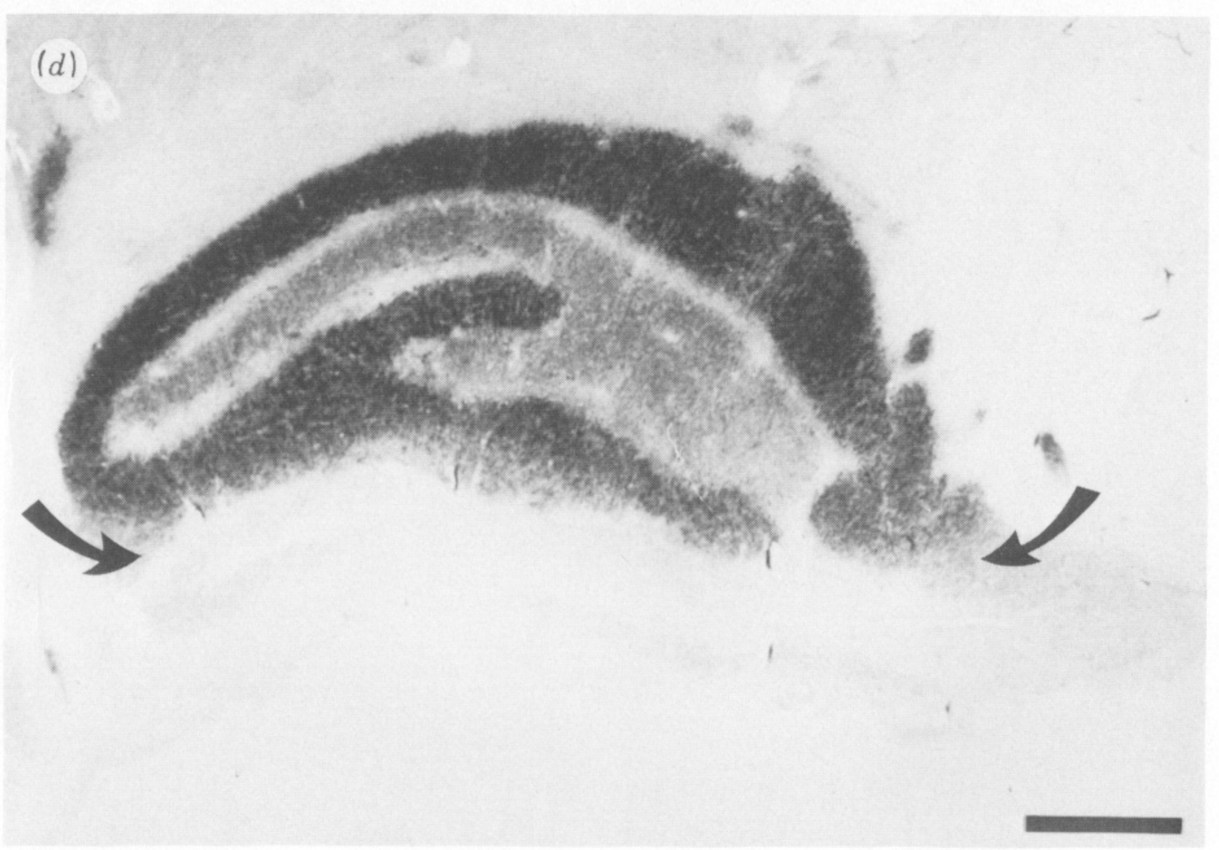

FIGURE 6. For description see p. 260.

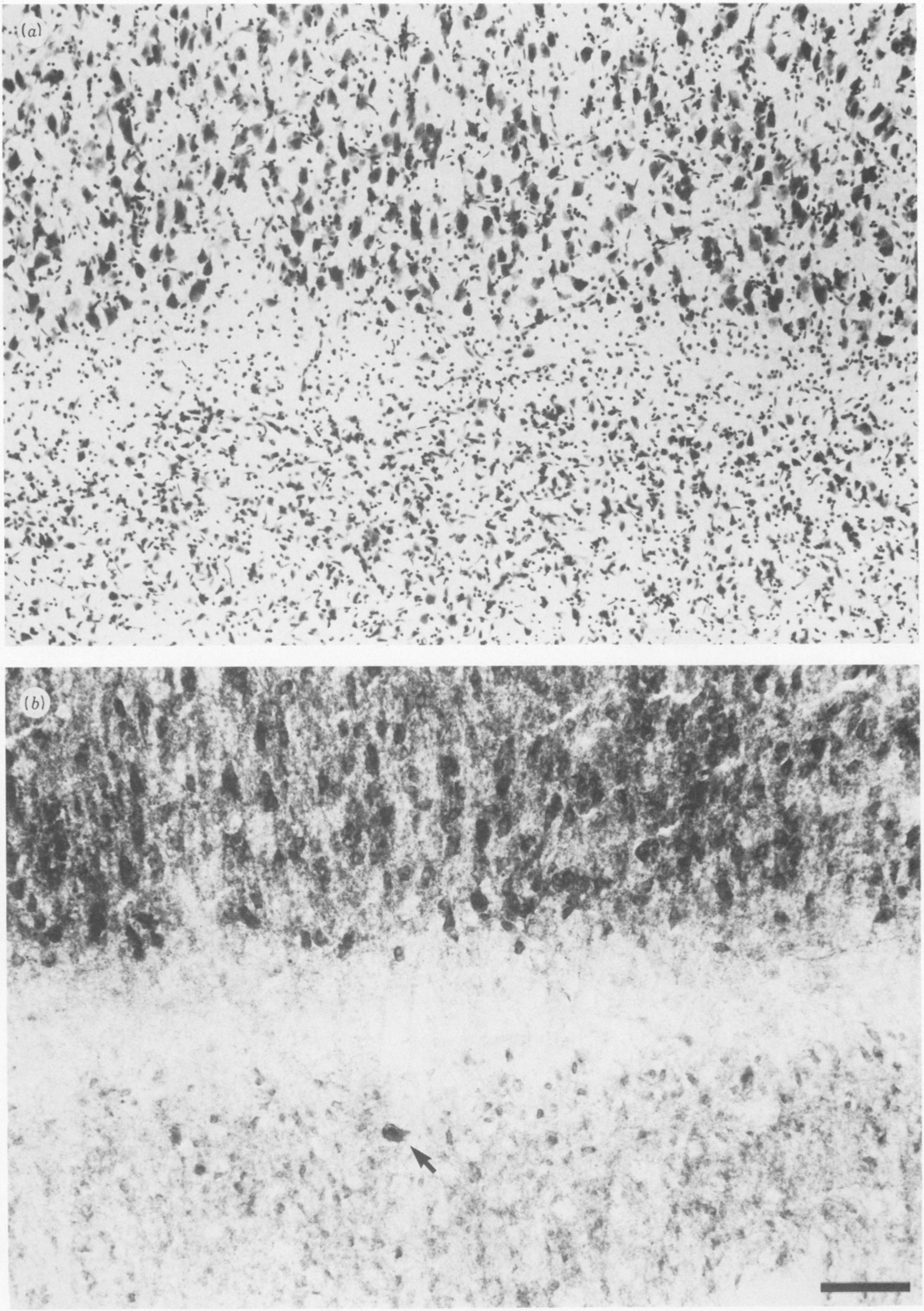

FIGURE 7. For description see p. 261.

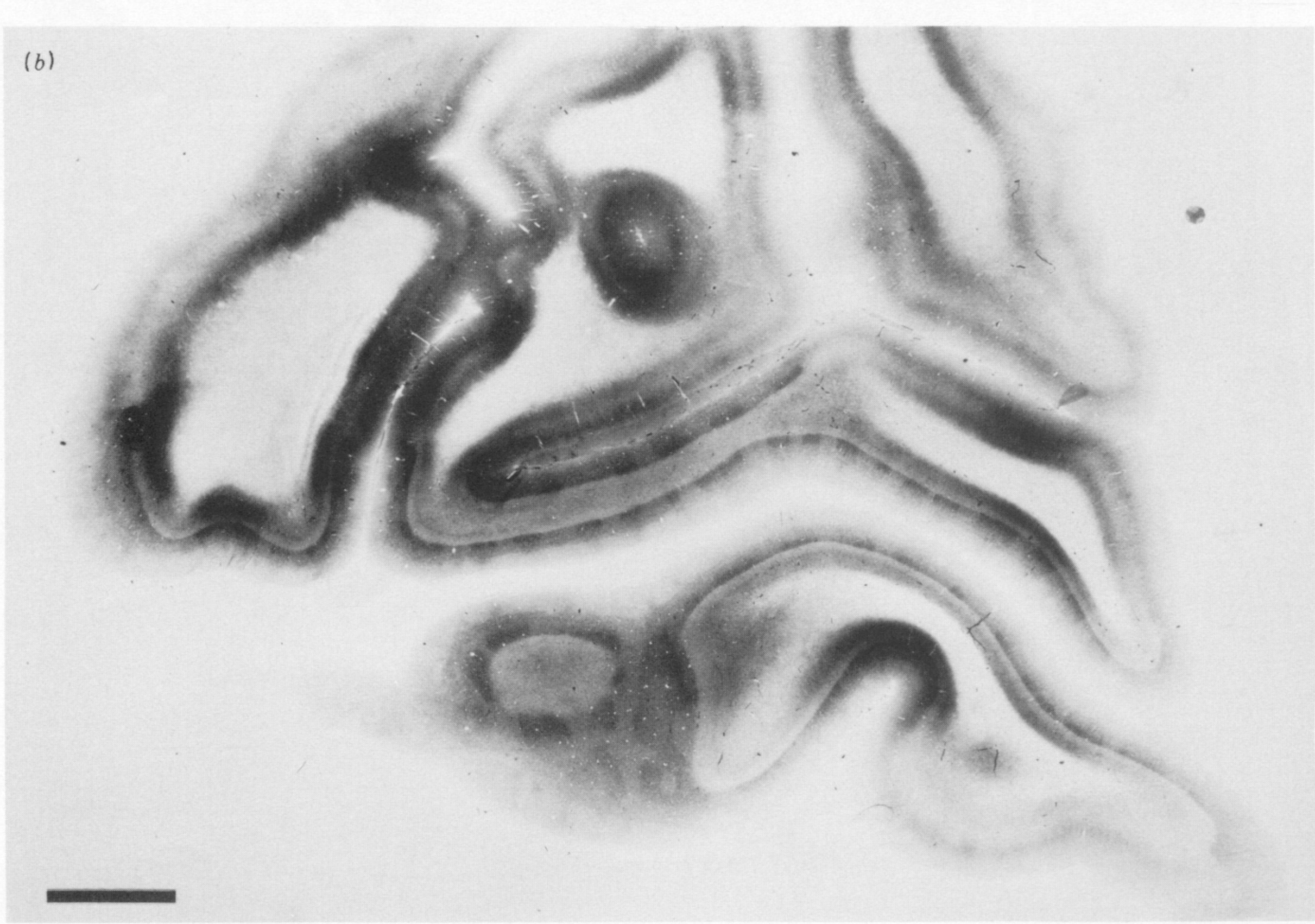

FIGURE 8. For description see p. 261.

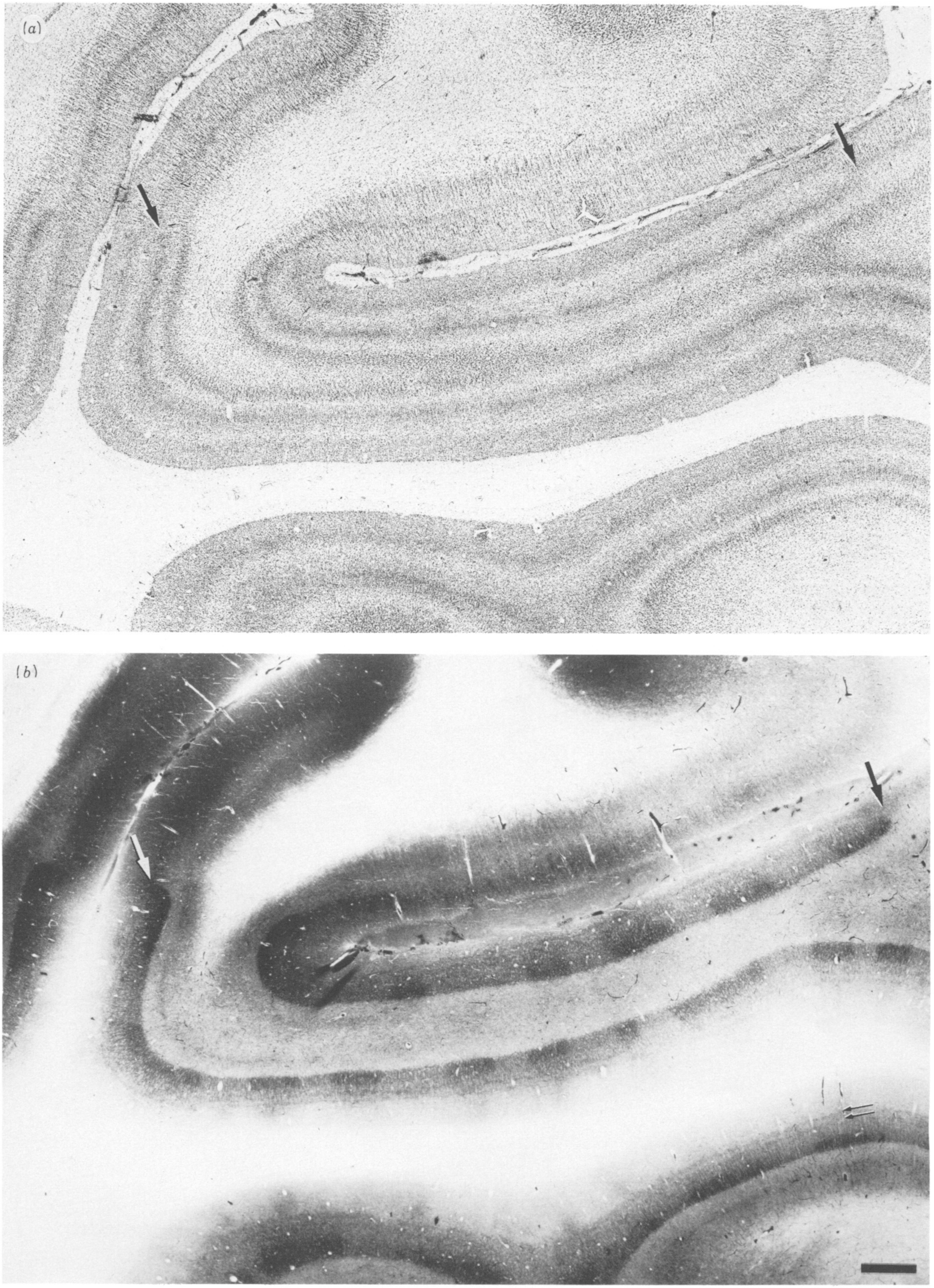

FIGURE 9. For description see p. 261.

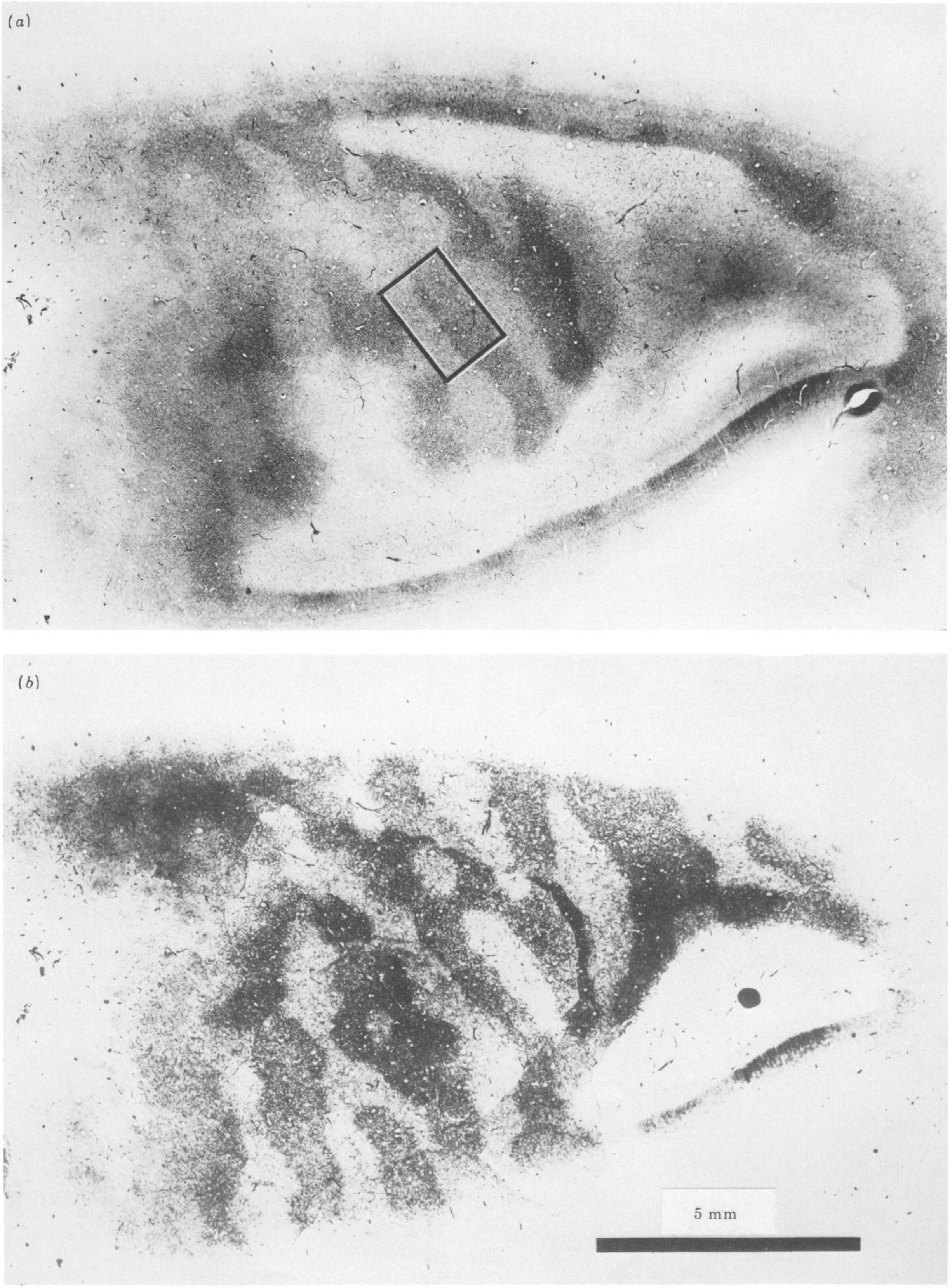

FIGURE 10. For description see opposite.

(a)

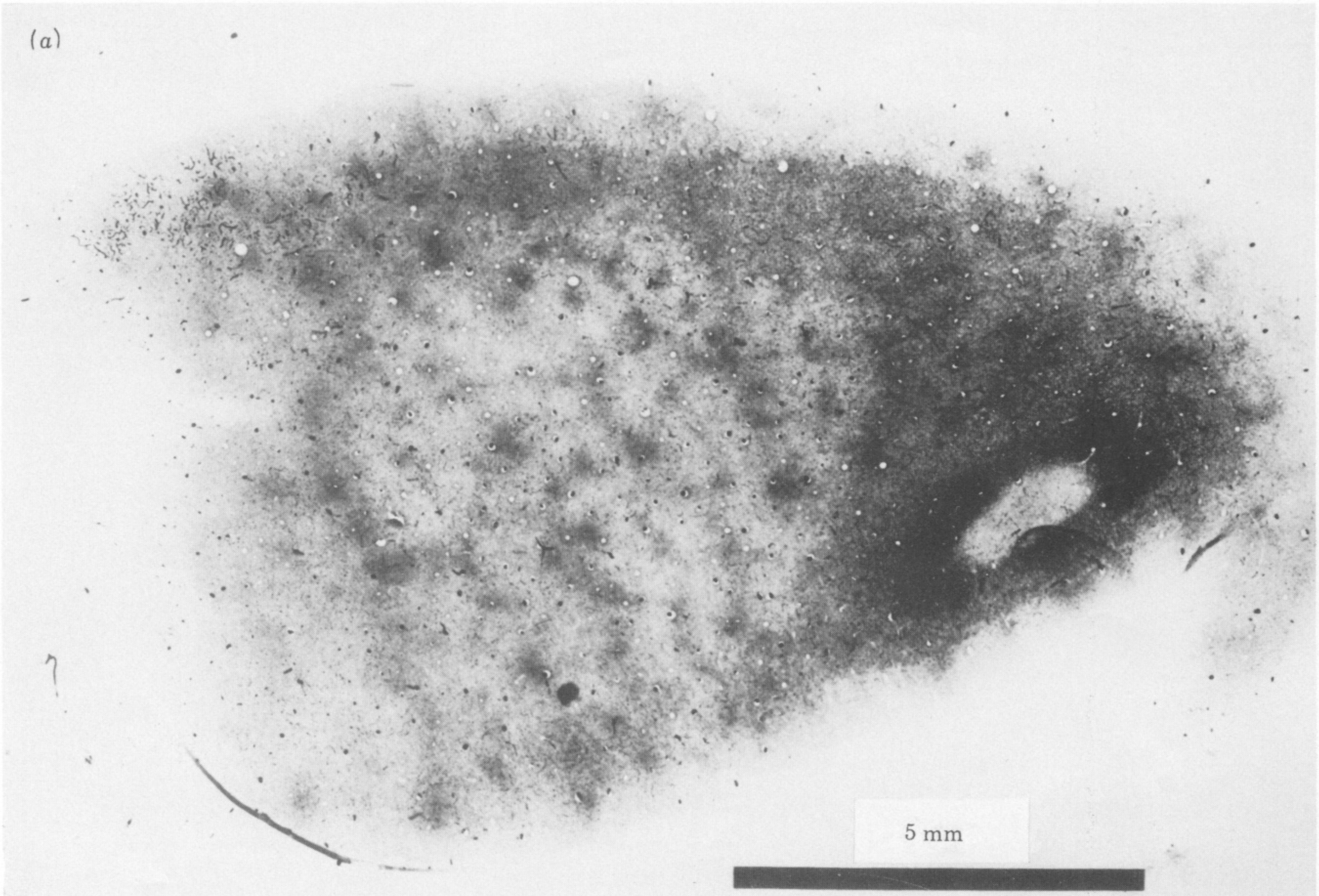

(b)

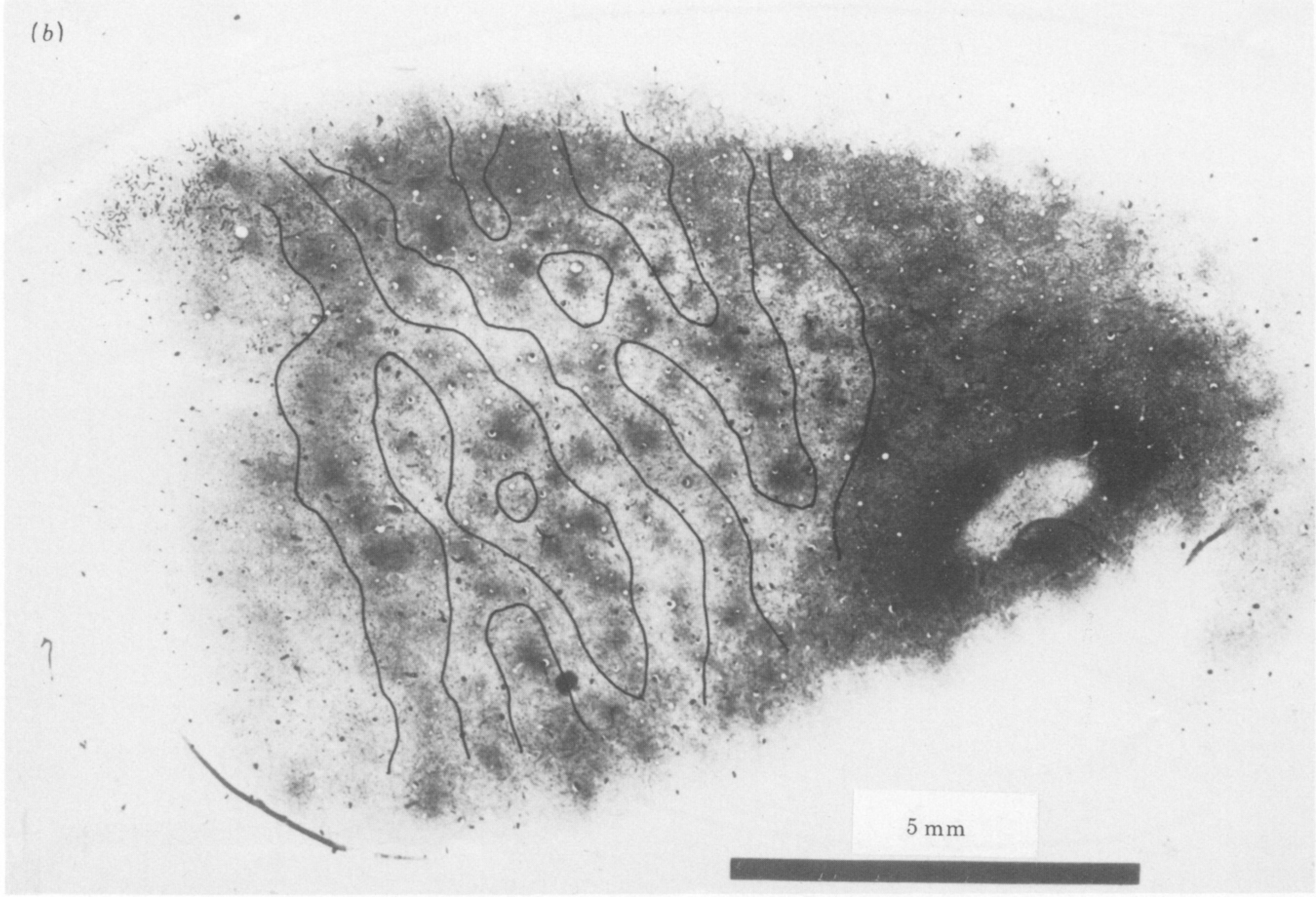

FIGURE 11. For description see opposite.

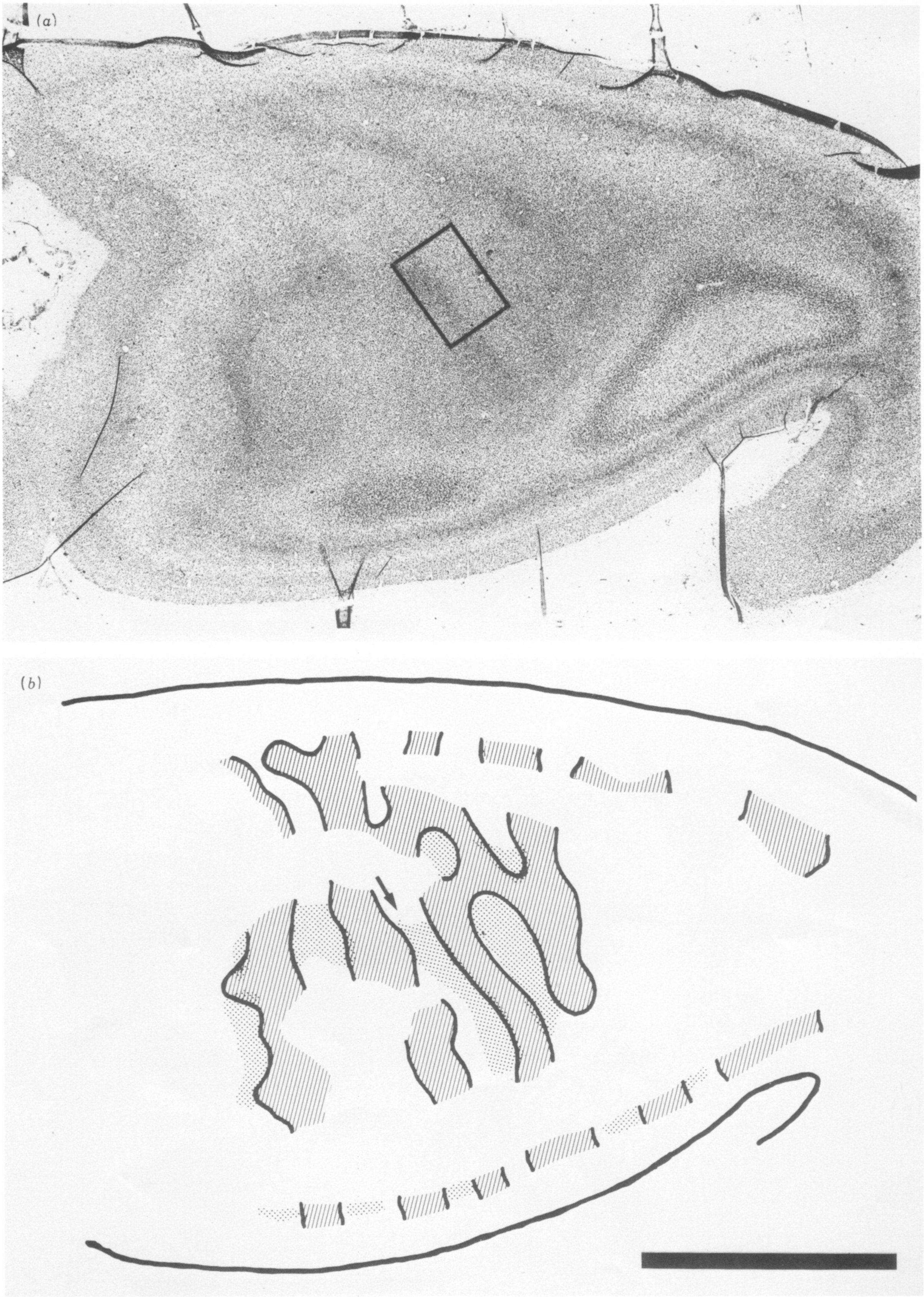

FIGURE 12. For description see p. 264.

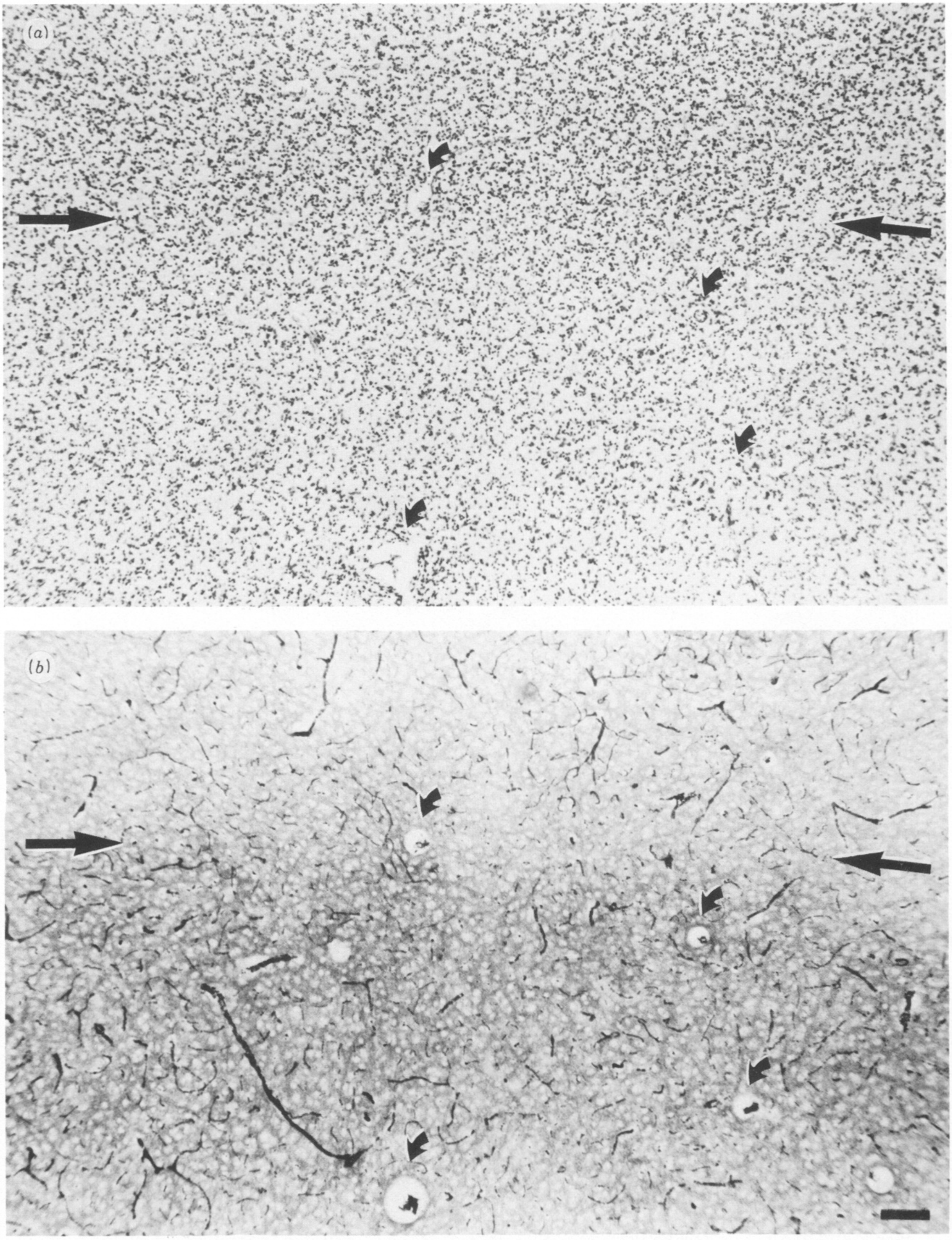

FIGURE 13. For description see p. 264.

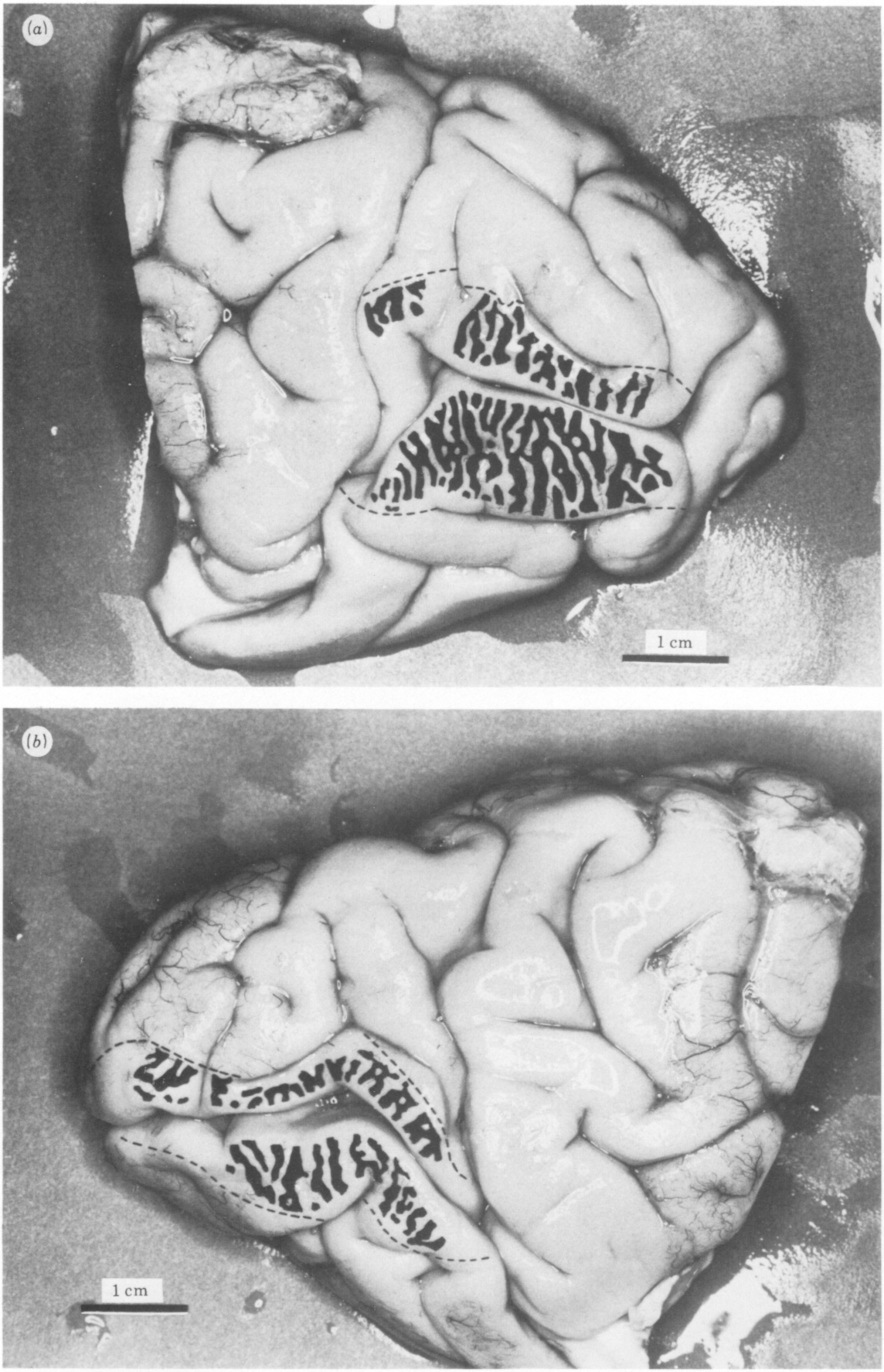

FIGURE 15. For description see p. 265.

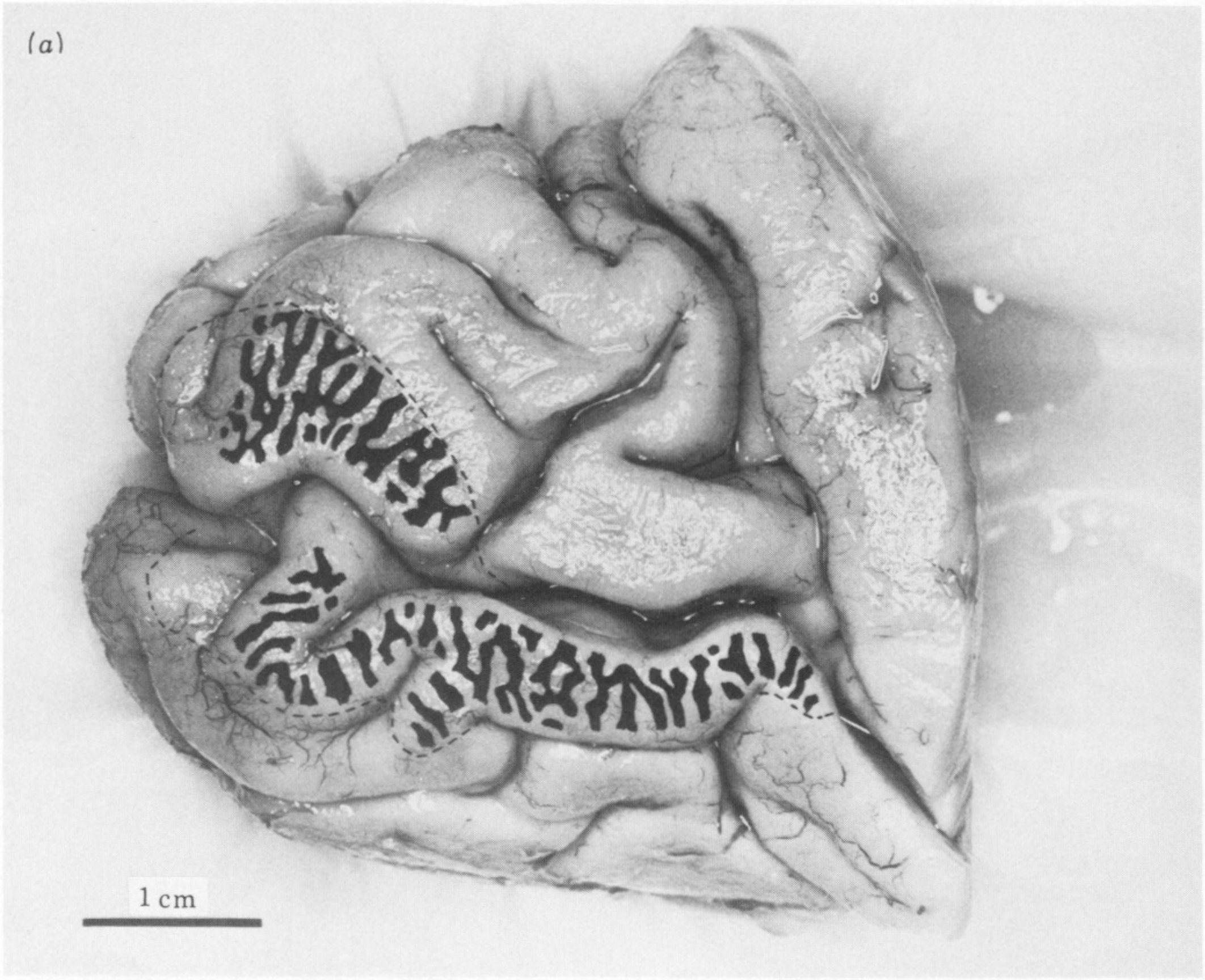

FIGURE 16. (*a*) Left and (*b*) right hemispheres from a 75 year old woman whose left eye was removed ten years before death showing superimposed pattern of ocular dominance columns in striate cortex. Again, columns are generally oriented perpendicular to the 17–18 boundary and appear as irregular slabs, averaging about 1 mm wide. Note how variable the pattern of sulci and gyri is from specimen to specimen: in (*b*) the calcarine sulcus is actually broken into two separate portions by a bridge of tissue.

17

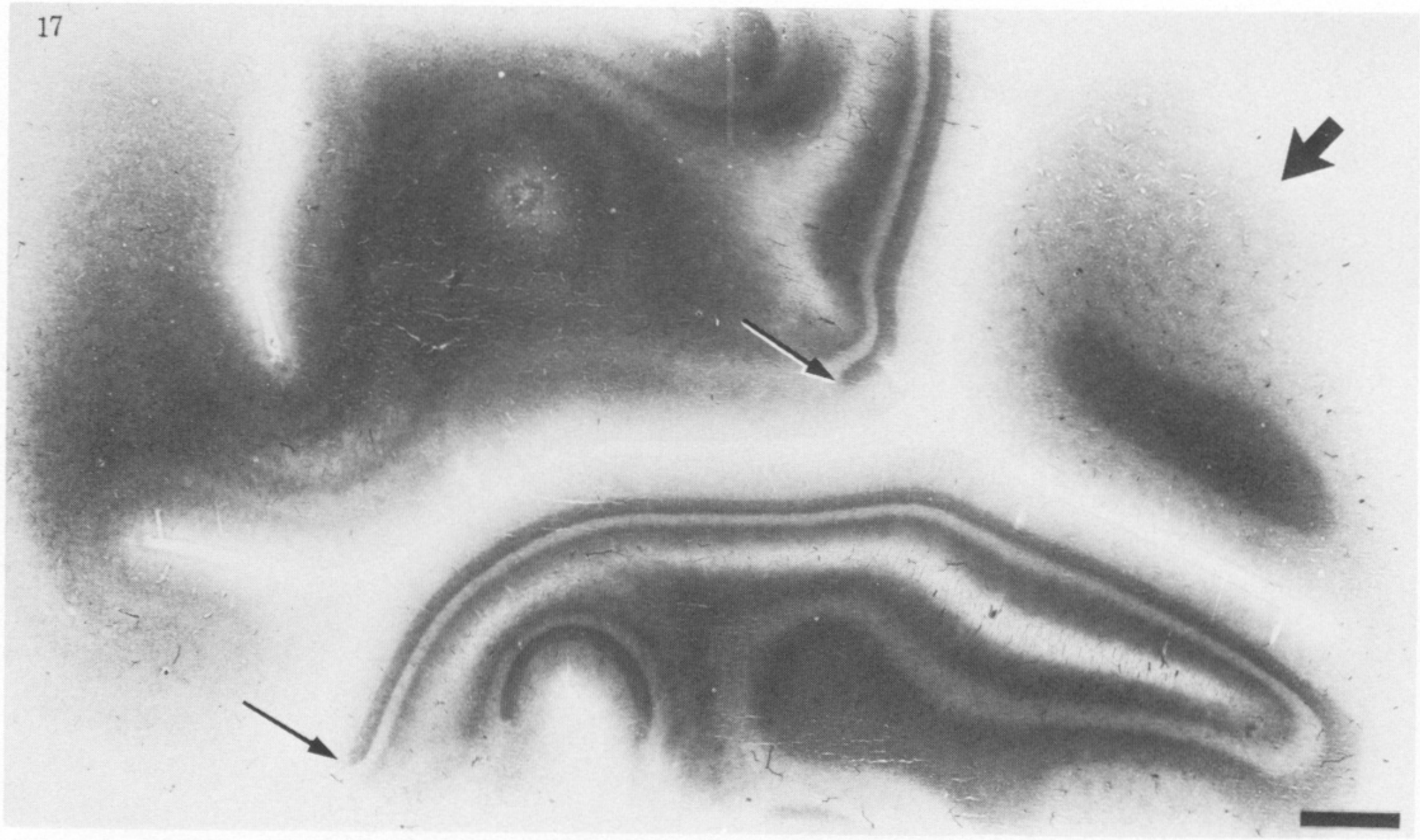

18*a*

18*b*

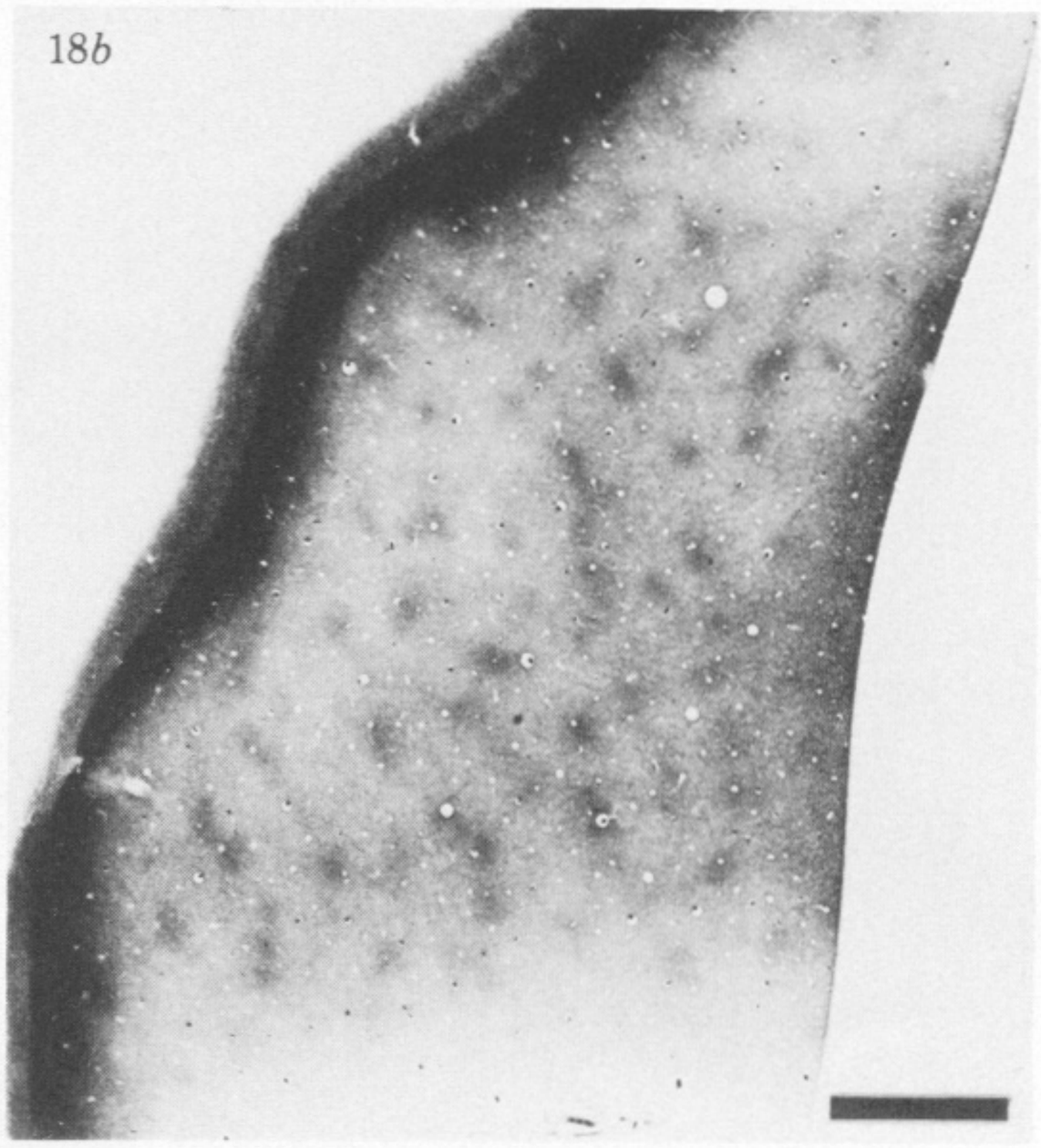

18*c*

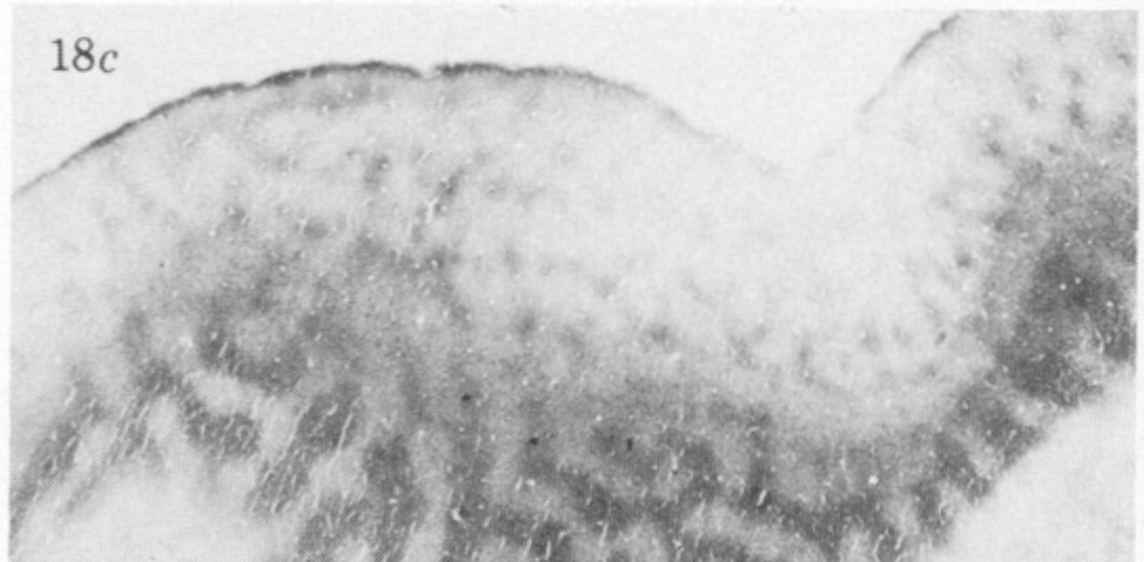

18*d*

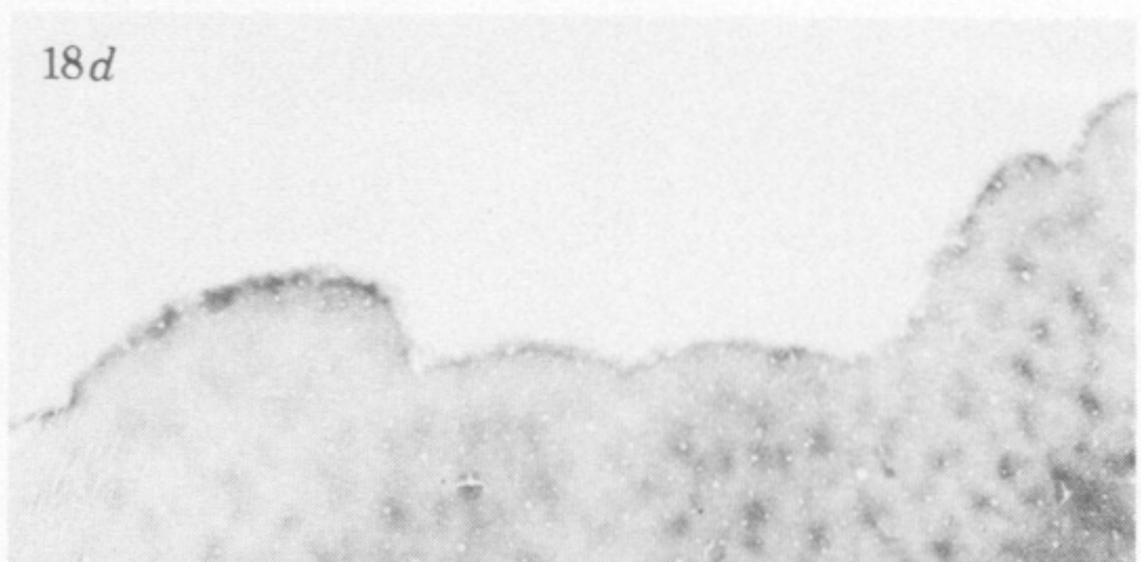

FIGURES 17 AND 18. For description see opposite.